

AD/A-003 755

MONOCHROMATIC TRANSMITTANCE/RADIANCE
COMPUTATIONS

Charles M. Randali

Aerospace Corporation

Prepared for:

Space and Missile Systems Organization
Defense Advanced Research Projects Agency

31 December 1974

DISTRIBUTED BY:

NTIS

National Technical Information Service
U. S. DEPARTMENT OF COMMERCE

UNCLASSIFIED

SECURITY CLASSIFICATION OF THIS PAGE (When Data Entered)

REPORT DOCUMENTATION PAGE		READ INSTRUCTIONS BEFORE COMPLETING FORM
1. REPORT NUMBER SAMSO-TR-74-247	2. GOVT ACCESSION NO.	3. RECIPIENT'S CATALOG NUMBER AD/A-003755
4. TITLE (and Subtitle) MONOCHROMATIC TRANSMITTANCE/ RADIANCE COMPUTATIONS		5. TYPE OF REPORT & PERIOD COVERED Interim
		6. PERFORMING ORG. REPORT NUMBER TR-0075(5647)-3
7. AUTHOR(s) Charles M. Randall		8. CONTRACT OR GRANT NUMBER(s) F04701-74-C-0075
9. PERFORMING ORGANIZATION NAME AND ADDRESS The Aerospace Corporation El Segundo, Calif. 90245		10. PROGRAM ELEMENT, PROJECT, TASK AREA & WORK UNIT NUMBERS
11. CONTROLLING OFFICE NAME AND ADDRESS Defense Advanced Research Projects Agency 1400 Wilson Boulevard Arlington, Va. 22209		12. REPORT DATE 31 December 1974
		13. NUMBER OF PAGES 86
14. MONITORING AGENCY NAME & ADDRESS (if different from Controlling Office) Space and Missile Systems Organization Air Force Systems Command Los Angeles, Calif. 90045		15. SECURITY CLASS. (of this report) Unclassified
		15a. DECLASSIFICATION/DOWNGRADING SCHEDULE
16. DISTRIBUTION STATEMENT (of this Report) Approved for public release; distribution unlimited		
17. DISTRIBUTION STATEMENT (of the abstract entered in Block 20, if different from Report)		
18. SUPPLEMENTARY NOTES Formerly ATM-74(4647)-6		
19. KEY WORDS (Continue on reverse side if necessary and identify by block number) Computer programs Atmospheric transmittance Radiative transfer Infrared Hot gases		
20. ABSTRACT (Continue on reverse side if necessary and identify by block number) A computer program and associated procedures have been developed to compute high resolution spectra for inhomogeneous optical paths including both atmospheric conditions and conditions typical of a missile plume. These programs and procedures are outlined in this report. The procedures have been used with the Air Force Cambridge Research Laboratories (AFCRL) line atlas to demonstrate that ignoring the correlation of atmospheric absorption lines with source emission lines can		

DD FORM 1473
(FACSIMILE)

UNCLASSIFIED

SECURITY CLASSIFICATION OF THIS PAGE (When Data Entered)

UNCLASSIFIED

SECURITY CLASSIFICATION OF THIS PAGE(When Data Entered)

19. KEY WORDS (Continued)

20. ABSTRACT (Continued)

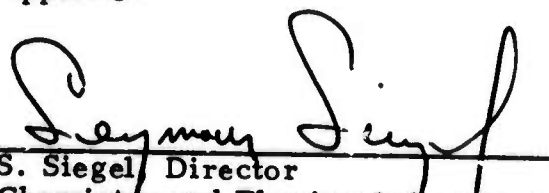
lead to errors as high as 79 percent for some spectral bands and optical paths. Calculated spectra have been compared with experimental laboratory spectra typical of both atmospheric and missile plume conditions. The AFCRL line atlas requires the addition of lines from highly excited states and the correction of certain inadvertent errors to be applicable to the calculation of high temperature optical properties of gases.

UNCLASSIFIED

SECURITY CLASSIFICATION OF THIS PAGE(When Data Entered)

This research was supported by the Defense Advanced Research Projects Agency of the Department of Defense and was monitored by Space and Missile Systems Organization (SAMSO) under Contract No. F04701-74-C-0075.

Approved


S. Siegel, Director
Chemistry and Physics Laboratory
Laboratory Operations

Publication of this report does not constitute Air Force approval of the report's findings or conclusions. It is published only for the exchange and stimulation of ideas.

ACCESSION for		
NTIS	Write Section	<input checked="" type="checkbox"/>
D C	Ref. Section	<input type="checkbox"/>
UNCLASSIFIED		<input type="checkbox"/>
JUSTIFICATION		
BY		
DISTRIBUTION/AVAILABILITY CODES		
DIST.	ATL.	ADD/SPECIAL
A		


GERHARD E. AICHINGER
Acting Chief
Contracts Management Office

CONTENTS

I.	INTRODUCTION	7
II.	QUASI-MONOCROMATIC TRANSMITTANCE/ RADIANCE COMPUTATION METHOD	11
A.	Introduction and Radiative Transport Equations	11
B.	Program Design	14
C.	Continuum Absorption/Transmittance	23
D.	Inhomogeneous Path Approximation	25
E.	Program Execution Time	28
III.	SOURCE SPECTRAL EFFECTS ON APPARENT ATMOSPHERIC TRANSMITTANCE	31
A.	Test Cases	31
B.	Atmospheric Transmittance Effective for Low Resolution Sensor	35
IV.	PROGRAM AND LINE ATLAS EVALUATION	43
A.	Comparison of Computed High Resolution Spectra and Experimental Results	43
B.	Atmospheric CO ₂ Path	43
C.	Atmospheric H ₂ O Path	48
D.	Hot CO ₂ Path	58
E.	Hot H ₂ O Path	60
V.	SUMMARY	63
	APPENDIX: USER'S GUIDE TO INHOM	65
1.	Introduction	65
2.	INHOM Program Control	66
a.	Introduction	66
b.	Step Definition Format	66
c.	Detailed Computation Step Definition	67

CONTENTS (Continued)

3.	Line Atlas Format	73
4.	Computer Compatible Output Format	75
5.	Sample Problem	75
REFERENCES		83

TABLES

1.	SPECPST Program Capabilities	15
2.	Partition Function Coefficients	22
3.	Selective Gas Line-Broadening Coefficients for H ₂ O and CO ₂	24
4.	Comparison of Segmenting Algorithms for Inhomogeneous Atmosphere	27
5.	Isothermal Typical Target Model	32
6.	Tropical Model Atmosphere	34
7.	Radiometer Transmittance	40
8.	Conditions for Experimental Comparison with Computed Spectra	44
A-1.	Frequency Range Covered by Each File on the Line Atlas Tape	73
A-2.	Parameters in Spectroscopic Line Atlas	74
A-3.	Logical Record Format for Spectrum Output Tapes	76

FIGURES

1.	Schematic Diagram of the Radiation Transport Problem Applicable to the Observation of Missiles through the Atmosphere	8
2.	Physical Relationships Required to Develop the Radiative Transfer Equation	12
3.	Schematic Diagram of the Procedure Employed to Compute the Effect of the Atmosphere on the Transport of Infrared Radiation	16
4.	Schematic Diagram of INHOM Program Operation	18
5.	Transmittance from 0 to 20 km at a 60-Deg Zenith Angle through a Mid-Latitude Summer Atmosphere	26
6.	Ratio of the Transmittance Computed with 5 Segments of Equal Air Molecule Content to the Transmittance Computed with 40 Segments of Equal Air Molecule Content	29
7.	Radiance from a Typical Target at 20 km	33
8.	Transmittance of the Atmosphere along a Path from 20 km to Space at a 75-Deg Zenith Angle through a Tropical Atmosphere	36
9.	Apparent Spectral Radiance of a Typical Target after Traversing a Path through the Atmosphere from 20 km to Space at a 75-Deg Zenith Angle	37
10.	Transmittance Computed in Several Ways for a Horizontal Path 100 km Long at 20 km Altitude	38
11.	Transmittance Computed in Several Ways for a Slant Path from 20 km to Space at a 75-Deg Zenith Angle	39
12.	Comparison of Computed CO ₂ Transmittance with Low Resolution Laboratory Experimental Observations Characteristic of Atmospheric Paths	45

FIGURES (Continued)

13.	Comparison of Computed CO ₂ Transmittance with High Resolution Laboratory Experimental Observations Characteristic of Atmospheric Paths	47
14.	Comparison of Computed H ₂ O Transmittance with High Resolution Laboratory Experimental Observations Characteristic of Atmospheric Paths	49
15.	Comparison of Computed CO ₂ Radiance with Laboratory Observations at High Temperature	59
16.	Comparison of Computed H ₂ O Transmittance with Laboratory Experimental Observations at High Temperature	61
A-1.	Sample Input Deck for INHOM Program Employing the Altitude Profile Method of Specifying the Atmosphere	77
A-2.	Spectrum Computed and Listing Generated by the INHOM Program in Response to the Input Deck Shown in Fig. A-1	78

I. INTRODUCTION

The spectrum of the source must be considered when attempting to correct observations of a source for the effects of absorption by the atmosphere between the source and the sensor. Computer programs capable of calculating transmittance and radiance over an inhomogeneous path at a spectral resolution fine enough to include individual line shapes have been developed to quantitatively study these source-dependent transmittance effects. Because these computer programs are applicable to a wide variety of additional problems involving radiation transport, their basis and use will be described in some detail. This will be followed by a presentation of results computed with the programs applied to the specific problem of quantitatively estimating the effect that the source spectrum can have on atmospheric transmittance corrections applicable to measurements from a sensor with spectral bandwidth greater than a single spectral line width.

The basic problem to which these programs have been applied in the present study is summarized in Fig. 1. A target with radiance L_t is viewed by a sensor through an atmospheric path. The idealized sensor indicates accurately the apparent radiance L_a arriving at its entrance aperture. A common objective of such measurements is to infer information about the source radiance from the observed apparent radiance. To achieve this objective, corrections for the effects of the intervening atmosphere must usually be made. The magnitude of these corrections depends on atmospheric conditions along the path from source to sensor and the spectral interval over which the sensor operates. Since most real sensors do not have a spectral resolution adequate to separate individual lines in the apparent radiance spectrum, these atmospheric corrections will also depend on the source spectrum and the spectral resolution of the sensor. In the infrared, these source-dependent factors can be particularly significant in cases where the source emission is due to hot carbon dioxide and water

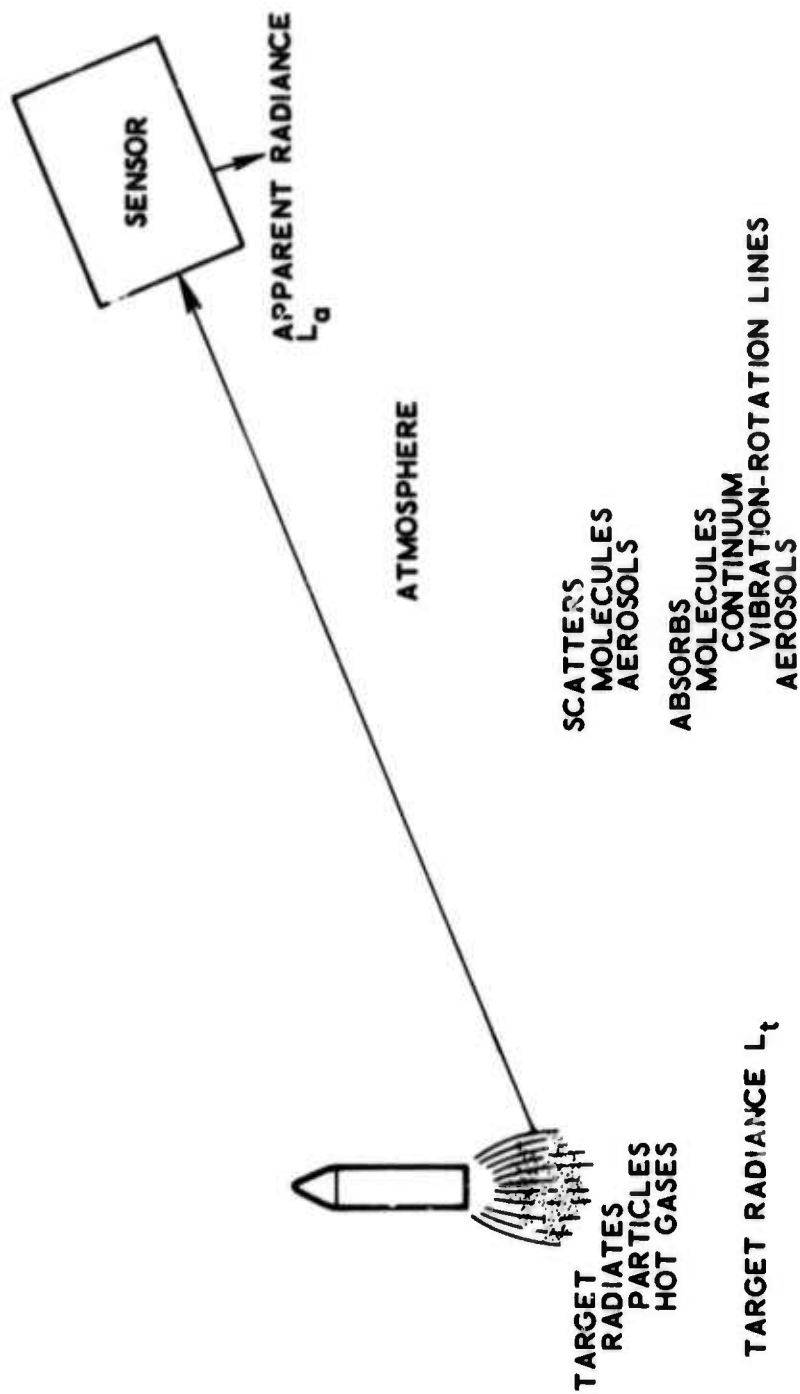


Fig. 1. Schematic Diagram of the Radiation Transport Problem Applicable to the Observation of Missiles through the Atmosphere

vapor, since these same gases are also responsible for the absorption of radiation by the atmosphere. Of course, radiation can occur from sources other than hot gases and be prevented from reaching the sensor by atmospheric processes other than molecular absorption. Some of these other processes are listed in Fig. 1, but they are not considered in detail in the present study since they are not expected to lead to significant source-dependent atmospheric transmittance corrections. The objects of the studies reported here are to: (a) demonstrate the magnitude of the dependence of atmospheric transmittance corrections on the source spectrum, (b) provide a means of computing these effects, (c) test and demonstrate the use of computer programs for the computation of high resolution transmittance and radiance spectra for inhomogeneous paths, and (d) test the validity of the AFCRL line atlas for hot gas spectral computations.

The source dependence of atmospheric transmittance corrections for finite spectral bandwidth sensors can be computed from quasi-monochromatic source radiance and atmospheric transmittance spectra. The unambiguous demonstration of such effects has been an objective of the present study. However, such quasi-monochromatic computations are much too time consuming for the routine reduction of data. For this reason, the development of a band model approach to the efficient computation of source-dependent transmittance spectra has been a part of the present study and is reported in Ref. 1. A second use of the quasi-monochromatic computations has been to examine the validity of this band model approach to source-dependent transmittance computations. This comparison is presented in Ref. 1.

The computer programs for radiation transport developed as part of this study are presented in some detail in Section II. These programs are applicable to a wide range of problems. Results obtained with these

¹ S. J. Young, Band Model Calculations of Atmospheric Transmittance for Hot Gas Line Emission Sources, TR-0075(5647)-1, The Aerospace Corporation, El Segundo, California (in preparation, June 1974).

computational tools are given in Section III. Section IV is devoted to a comparison of computed values with experimental observations to ascertain the applicability of the input spectroscopic data and the accuracy of the programs.

II. QUASI-MONOCHROMATIC TRANSMITTANCE/ RADIANCE COMPUTATION METHOD

A. INTRODUCTION AND RADIATIVE TRANSPORT EQUATIONS

The problem of particular interest in this study, namely, the computation of the source spectral dependence of effective atmospheric transmittance, is a particular type of radiative transfer problem. In studying such problems on a quasi-monochromatic basis (as is done in this study), complexities arise as a result of the masses of data required rather than from the involved mathematical equations that describe the transport of radiation. The basic radiation transport equation relating for a single frequency ν the radiance $L_t(\nu)$ at location 0 to the radiance $L_a(\nu)$ at the sensor depends on the transmittance and radiance of incremental slabs of the intervening atmosphere. Referring to Fig. 2,

$$L_a(\nu) = L_t(\nu) T_{0,D}(\nu) + \sum T_{z_i,D}(\nu) \sigma_i(\nu) \quad (1)$$

where

$$T_{z_m, z_n} = \prod_{i=m}^{i=n} \tau_i = \exp \left[- \int_{z_m}^{z_n} k(\nu, z) dz \right] \quad (2)$$

These equations can also be written in integral form, but the discrete sum and product form is directly applicable to implementation on a digital computer and so will be retained. Along an atmospheric path for which infrared absorption is significant, it is usually possible to assume that collisions

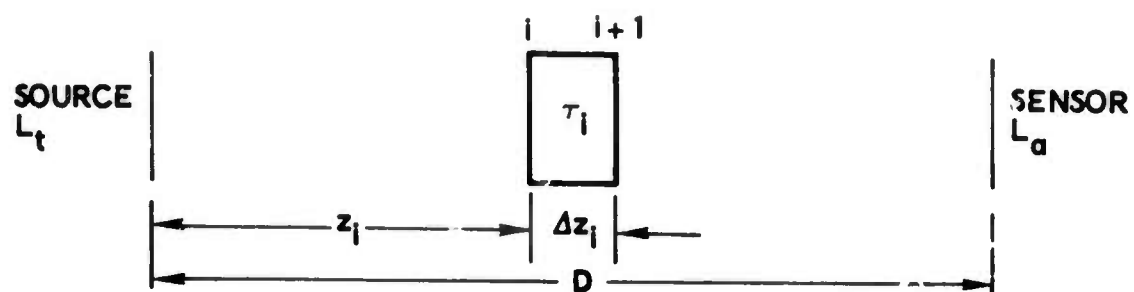


Fig. 2. Physical Relationships Required to Develop the Radiative Transfer Equation

between molecules occur frequently enough for a temperature to be defined, and thus the gas is in local thermodynamic equilibrium. The temperature then determines the distribution of energy among the quantum states of the molecule. In this case, the radiance of an atmospheric segment is

$$\sigma_i(\nu) = [1 - \tau_i(\nu)] L_b(\nu, \theta) \quad (3)$$

where $L_b(\nu, \theta)$ is the radiance at frequency ν of a blackbody at temperature θ . For this case, the radiation transport problem requires only the computation of the transmittance $\tau_i(\nu)$ for the segments along the optical path.

When Eqs. (1) and (3) are combined,

$$L_a(\nu) = L_t(\nu) T_{0,D}(\nu) + \sum_{i=1}^N T_{z_i,D}(\nu) [1 - \tau_i(\nu)] L_b(\nu, \theta) \quad (4)$$

Equations (2) and (4) form the basis for computer calculation of the transport of radiation through inhomogeneous atmospheres. The Aerospace Corporation radiation transport computer program, INHOM, discussed in more detail in paragraph II. B employs these equations to approximate inhomogeneous paths by up to 81 homogeneous segments.

The transmittance of individual segments can be computed from spectroscopic information about the strength and width of the spectral lines resulting from the various possible transitions between the energy levels of the molecules in the optical path. In the infrared region, these transitions are normally between various vibration-rotation states. There are usually a large number of possible transitions. Only with the recent appearance of the compilation of line parameters obtained under the direction of R. A. McClatchey of the Air Force Cambridge Research Laboratories

(AFCRL)² has there been available the necessary spectroscopic information organized in a fashion to facilitate the computation of atmospheric spectra.

The AFCRL line atlas, described in detail in Ref. 2, provides spectroscopic data for more than 110,000 infrared transitions of the 7 gases: H_2O , CO_2 , O_3 , N_2O , CO , CH_4 , and O_2 . For each transition, the strength S_i^0 and line width α_i^0 at 1-atm pressure and 296 K are provided along with the lower energy level E_i^0 of the transition and the quantum numbers specifying the energy levels between which the transition takes place. These are arranged in the order of ascending transition frequency ν_i for convenience in spectral calculations. This organization mixes the transitions of various molecules so that the molecule must also be indicated for each line.

An efficient, but flexible, computer program operating on a fast digital computer is required to utilize any spectroscopic line atlas, such as the AFCRL compilation, for calculations covering an appreciable spectral interval. Our approach to such a computer program, designed for use on the Control Data 7600 high speed computer available at The Aerospace Corporation, is described in the remainder of this section.

B. PROGRAM DESIGN

Equation (4) has been written separating the source radiance from the atmospheric effects. It is useful to maintain this separation of the radiative transport equation into source and atmospheric terms, as is implied by Eq. (4), in the actual computation of spectra since it is often desired to study the spectrum resulting from the transmittance of radiance from the same source through a variety of optical paths or, conversely, the transmittance of various sources through the same optical path. This separation

²R. A. McClatchey, W. S. Benedict, S. A. Clough, D. E. Burch, R. F. Calfee, K. Fox, L. S. Rothman, and J. S. Garing, AFCRL Atmospheric Absorption Line Parameters Compilation, Environmental Research Paper 434, AFCRL-TR-73-0096, Air Force Cambridge Research Laboratories, Mass. (26 January 1973).

then becomes desirable because the combination of source and transmittance spectra can be done much more rapidly than the computation of the spectra. The combination operations are performed by a modified version of an existing program that also has the capability to produce plots and convolve instrument functions with the combined spectra. Figure 3 is a schematic diagram of the procedure employed to compute the apparent radiance of a target after the radiation has passed through the atmosphere. In this procedure, the INHOM Program computes quasi-monochromatic spectra based on path parameters input by punched cards to the program. It obtains spectroscopic data from the AFCRL line atlas, and the resulting spectra are then combined by the SPECST Program. The capabilities of SPECST are listed in Table 1 and described in detail in Ref. 3* and, therefore, are not delineated in this report.

Table 1. SPECST Program Capabilities

- | | |
|---|---|
| • | Combine spectra to create composite spectra. |
| • | Convolve spectra with defined sensor functions. |
| • | Compute average spectral values. |
| • | Print spectral values in convenient format. |
| • | Plot spectra for desired regions. |

Although different versions of the INHOM Program are shown in Fig. 3 for atmospheric and source computations, the programs differ only in the subroutines that calculate the absorptance of the segments. The relatively high temperatures and absorber concentrations in typical plumes require that a number of factors that are near unity for atmospheric spectra must

* This describes the basic SPECST Program only and does not include the modifications required to study INHOM produced spectra.

³ C. M. Randall, User's Guide to Computer Programs for Fourier Spectroscopy, TR-0073(9260-01)-8, The Aerospace Corporation, El Segundo, California (30 November 1972).

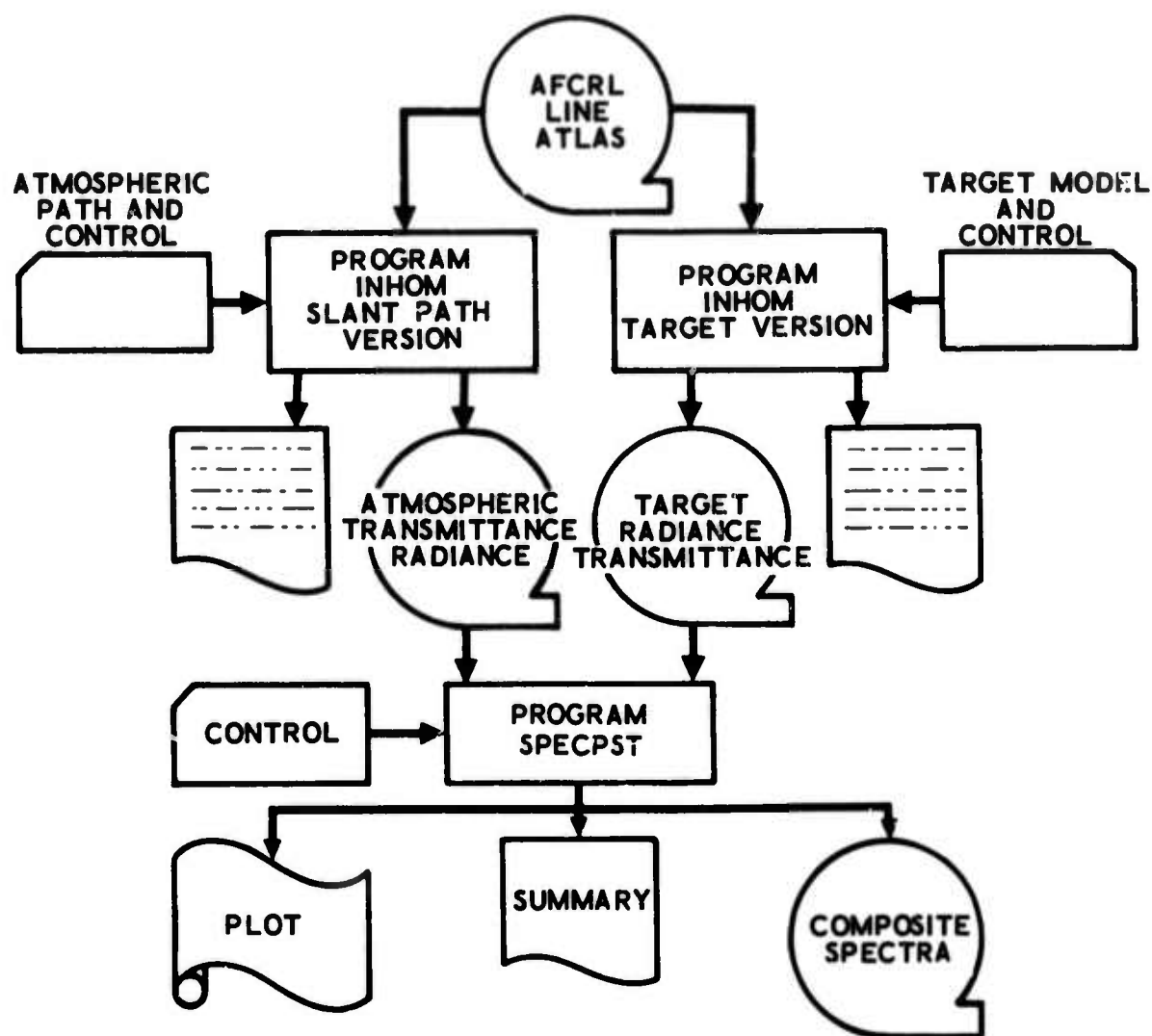


Fig. 3. Schematic Diagram of the Procedure Employed to Compute the Effect of the Atmosphere on the Transport of Infrared Radiation (The INHOM Program computes the quasi-monochromatic transmittance and radiance. The SPEC PST Program has the capability to: combine two or more spectra, convolve spectra with instrumental functions, and display the results in convenient printed and/or plotted form.)

be specifically included in the source spectrum calculation. A more detailed description of the INHOM transmittance/radiance program and its use is given in the following paragraphs.

A radiative transfer program should be flexible to allow its application to a wide variety of problems. At the same time, however, it should be fast to allow economical computing. Satisfaction of these two somewhat contradictory goals in the INHOM Program is attempted by separating the various required types of calculations into subprogram modules. The modules in which calculations are performed that are not repeated often, e.g., the transformation of atmospheric parameters into parameters characterizing the various segments along the optical path, have been made very flexible and general with only minor thought given to computation efficiency. On the other hand, those modules used frequently, e.g., to compute the line shape and absorption coefficient, have been optimized for efficient execution, even to the extent of assembly language coding. Flexibility for these computations is achieved by substituting a different version of the entire module.

The basic operation of the INHOM Program is indicated schematically in Fig. 4, and details of the program control required to utilize the various options are discussed in the Appendix. Control cards are read giving the program information until a SPECTRUM control card is encountered in the input stream. This card initiates the computation of a spectrum. The spectrum computed depends on information communicated on the SPECTRUM card and on other control cards encountered previously in the input stream. The optical path must be specified prior to the SPECTRUM step and this may be done in two ways. It may be specified directly by giving the column density of each gas in each segment along with the temperature, pressure, and path length characterizing that segment, or it may be specified indirectly by describing an atmosphere in terms of altitude profiles of temperature, pressure, and variable gas concentration. The program then converts these profiles into segment parameters by employing the geometric path

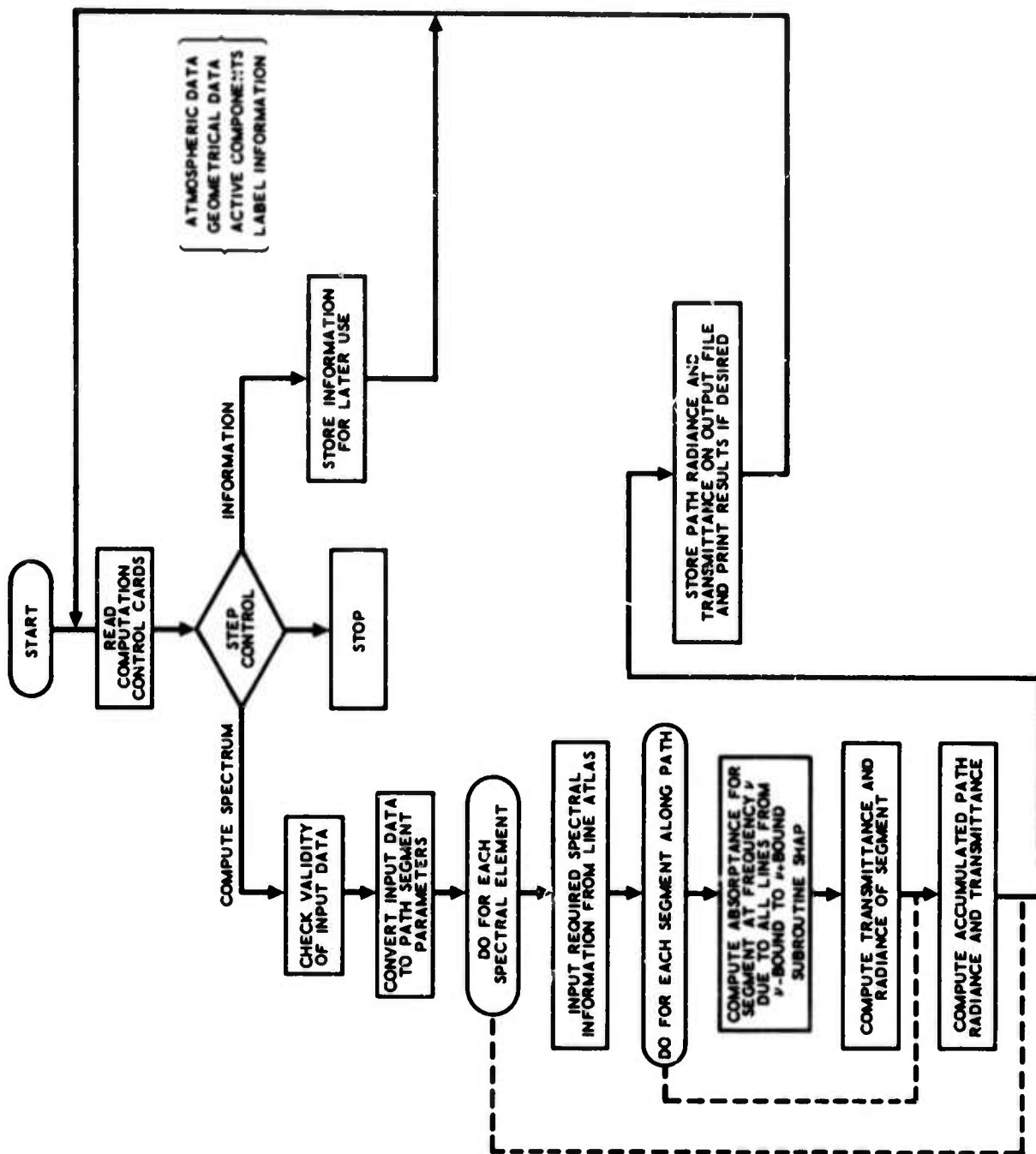


Fig. 4. Schematic Diagram of INHOM Program Operation

parameters designated by the user. This conversion neglects refraction effects, and assumes a round earth with a radius of 6378.16 km surrounded by symmetric shells of atmosphere. The path is specified by giving the zenith angle of the path at the beginning altitude and the final altitude. Paths with zenith angles greater than 90 deg are acceptable. If the final altitude is less than the beginning altitude, two paths are possible, and the user may select either one. All paths that intersect the earth's surface are recognized, and the computation of such a spectrum is prevented and an appropriate error message is printed. Paths entirely outside the atmosphere are also recognized, not computed, and an error message is printed.

The conversion of an inhomogeneous path to a collection of homogeneous segments may be done with a number of different assumptions. Only a limited amount of study has been given to the optimum way in which this should be done, but results obtained to date are reported in paragraph II.D.

After the optical path is properly specified, computation of the radiation transport equation begins. This computation is indicated by the DO statements in Fig. 4. Computation of the attenuation in a single segment for a single frequency is done in a subroutine called SHAP that can easily be changed to accommodate different line-shape functions.

The attenuation $k(\nu)$ computed by the SHAP subroutine for a single frequency ν is dependent on the contribution of many lines in the neighborhood of ν .

$$k(\nu) = \sum_{i=I_L}^{i=I_U} S_i W_i f[(\nu - \nu_i), \alpha_i] \quad (5)$$

where I_L and I_U are indices bracketing all the lines assumed to be close enough to ν to influence $k(\nu)$; S_i is the strength of the i th line; α_i is the width

of the i th line; $f[(\nu - \nu_i), \alpha_i]$ is a line-shape function; and W_i is the column density of the gas for which S_i and α_i characterize a line. The factors S_i and α_i are dependent on the pressure, temperature, and species concentration in the particular segment. All studies to date have been carried out assuming a Lorentz pressure-broadened line-shape function.

$$f[(\nu - \nu_i), \alpha_i] = \frac{\alpha_i}{\pi} [(\nu - \nu_i)^2 + \alpha_i^2]^{-1}$$

The line width and strength parameters depend on the molecule and the conditions in the segment of the optical path being considered. The AFCRL line atlas tabulates the line strengths and widths for $P_0 = 1$ atm and $\theta_0 = 296$ K temperature. Quantities drawn from the atlas are indicated by a superscript 0. In most of the calculations reported here, line strengths and widths appropriate to the path segments have been obtained by the following relations:

$$S_i = \frac{S_i^0 g(\nu, \theta) \exp \left[\frac{h E_i^0}{k} \left(\frac{1}{\theta_0} - \frac{1}{\theta} \right) \right]}{Q_v(\theta, m_i) Q_r(\theta, m_i)} \quad (6)$$

$$\alpha_i = \alpha_i^0 (P/P_0) (\theta_0/\theta)^{1/2} \quad (7)$$

where P and θ are the average pressure and temperature in a particular segment of the optical path, and h and k are the Planck constant and the Boltzmann constant, respectively. The correction for stimulated emission is

$$g(\nu, \theta) = 1 - \exp(-h\nu/k\theta) \quad (8)$$

For the spectral regions presently of interest, this correction differs significantly from unity only for the high temperatures involved in source radiance computations. The term E_i^0 is the energy of the lower energy level of the transition, and $Q_v(\theta, m_i)$ and $Q_r(\theta, m_i)$ are respectively the ratio of the vibrational and rotational partition function at temperature θ for the molecule m_i to the value of the partition function at $\theta_0 = 296$ K. For atmospheric conditions, Q_v differs only slightly from unity; thus, in many of the calculations for atmospheric paths reported here it has been assumed to be unity. The rotational partition function ratio $Q_r(\theta, m_i)$ is approximated by

$$Q_r(\theta, m) = (\theta/\theta_0)^{j_m} \quad (9)$$

where the value of the exponent depends on the molecule being considered. The values used are listed in Table 2 (Ref. 2). For source conditions, the vibrational partition function cannot be ignored and has been calculated in the harmonic approximation.⁴

$$Q_v(\theta, m) = \prod_j [1 - \exp(-hE_j^v/k\theta)]^{-d_j} \quad (10)$$

where E_j^v is the energy of the j th fundamental vibrational level and d_j is the degeneracy associated with that level. The coefficients employed are listed in Table 2.^{2, 4}

The theory of line broadening is complex and not totally adequate. For atmospheric conditions, the simple approximation of Eq. (7) has been employed. However, for source calculations, the concentration of certain

⁴G. Herzberg, Molecular Spectra and Molecular Structure, Van Nostrand Reinhold Company, New York, New York (1945), p. 501.

Table 2. Partition Function Coefficients

Gas	Rotational Function Exponent, j_m	Vibrational Fundamentals, E_j^v (cm^{-1})	Degeneracy, d_j
H_2O	1.5	1594.736 3657.054 3755.924	1 1 1
CO_2	1.0	667.379 1388.187 2349.146	2 1 1
O_3	1.5	Not included in source spectra $Q_v = 1$	
N_2O	1.0	Not included in source spectra $Q_v = 1$	
CO	1.0	Not included in source spectra $Q_v = 1$	
CH_4	1.5	Not included in source spectra $Q_v = 1$	
O_2	1.0	Not included in source spectra $Q_v = 1$	

species may be high enough for self-broadening to be significant. For these cases, we have used the results of Ludwig *et al.*⁵ to compute the broadening coefficient to be applied to the line width parameter $\alpha_{i,m}^0$ from the AFCRL atlas for the i th line of species m .

$$\alpha_{i,m} = \alpha_{i,m}^0 \left\{ \sum_j \gamma_m^j p_j (\theta_0/\theta)^{1/2} + \gamma_m^* p_m (\theta_0/\theta) \right\} / \gamma_m^0 \quad (11)$$

where γ_m^j is the broadening coefficient for gas j on gas m ; p_j is the partial pressure of gas j ; γ_m^* is the resonant self-broadening coefficient; and γ_m^0 is the result of carrying out the computation within the braces for dry air at $\theta_0 = 296$ K and a total pressure of $P_0 = 1$ atm. These are the conditions for which the AFCRL atlas line widths are calculated. For computational economy, the coefficients actually used are $\bar{\gamma}_m^j = \gamma_m^j / \gamma_m^0$. All of the relevant coefficients based on Ref. 5 are listed in Table 3.

C. CONTINUUM ABSORPTION/TRANSMITTANCE

All absorption mechanisms that vary only slightly on a spectral scale of a few line widths have been ignored in the present calculations, since the objective of the present study is to explore the effects of line correlation on apparent atmospheric transmittance. However, capabilities have been incorporated into the INHOM Program to include such phenomena when desired by generating an appropriate subroutine module.

The choice of an appropriate bound to place on the region over which lines influence the absorptance at frequency ν , I_L and I_U in Eq. (5), can be viewed as a decision on where to begin to include line wings as a continuum phenomenon to be handled by semiempirical means rather than by consideration of the explicit shape of individual lines. These line-shape functions are

⁵ C. B. Ludwig, W. Malkmus, J. E. Reardon, and J. A. L. Thomson, Handbook of Infrared Radiation from Combustion Gases, NASA Special Publication NASA SP-3080 (1973).

Table 3. Selective Gas Line-Broadening Coefficients for H₂O and CO₂

Colliding Gas \ Absorbing Gas	H ₂ O		CO ₂	
	$\bar{\nu}_i^j$ (cm ⁻¹ atm ⁻¹)	$\bar{\nu}_i^j$ (atm ⁻¹)	$\bar{\nu}_i^j$ (cm ⁻¹ atm ⁻¹)	$\bar{\nu}_i^j$ (atm ⁻¹)
H ₂ O	0.09	1.1782	0.07	1.073
CO ₂	0.12	1.571	0.09	1.3796
O ₂	0.04	0.5236	0.06	0.9197
N ₂	0.09	1.1782	0.07	1.073
Resonant Self-broadening	0.44	5.760	Not applicable	

probably not correct at great distances from the line center. An appropriate bound may be chosen by assuming that a Lorentz line shape is typical and noting that, under atmospheric conditions, line widths are 0.1 cm^{-1} or less. The rate of change of absorptance then decreases to less than 1 percent/ cm^{-1} beyond 10 cm^{-1} from the line center. With such rates of absorptance change, line correlation effects will be minimal; thus, we have adopted a limit of 10 cm^{-1} away from a frequency ν for the inclusion of line effects.

D. INHOMOGENEOUS PATH APPROXIMATION

The use of a series and continued product formulation for the radiation transport equation in an inhomogeneous medium, as defined in Eqs. (2) and (4), implies physically that the continuously varying path is being approximated by a series of homogeneous segments. The way in which the path is divided into homogeneous segments and the number of segments can affect the accuracy of the computed results. As a part of the present study, a limited variety of possible path division algorithms have been tried.

Division of the inhomogeneous path into equal geometric length segments and into segments containing equal numbers of air molecules has been tried. For each division scheme, a slant path through a mid-latitude summer model atmosphere from 0 to 20 km at a zenith angle of 60 deg has been divided into from 1 to 40 segments. Then, for each division scheme and each number of segments, the transmittance was computed in the 15 cm^{-1} band from 3400 to 3415 cm^{-1} with a resolution of 0.02 cm^{-1} . This spectral region was chosen because it contains a range of transmittances from 0.22 down to less than 10^{-4} . A spectrum computed for 40 segments is shown in Fig. 5. The transmittance spectra resulting from various runs are compared in two ways in Table 4. First, the average transmittance over the entire 15 cm^{-1} band for the various number of segments was compared with the result for 40 segments. Second, the individual transmittance spectra were divided by the 40-segment transmittance spectrum for all values for which the transmittance was greater than 10^{-4} . In the typical

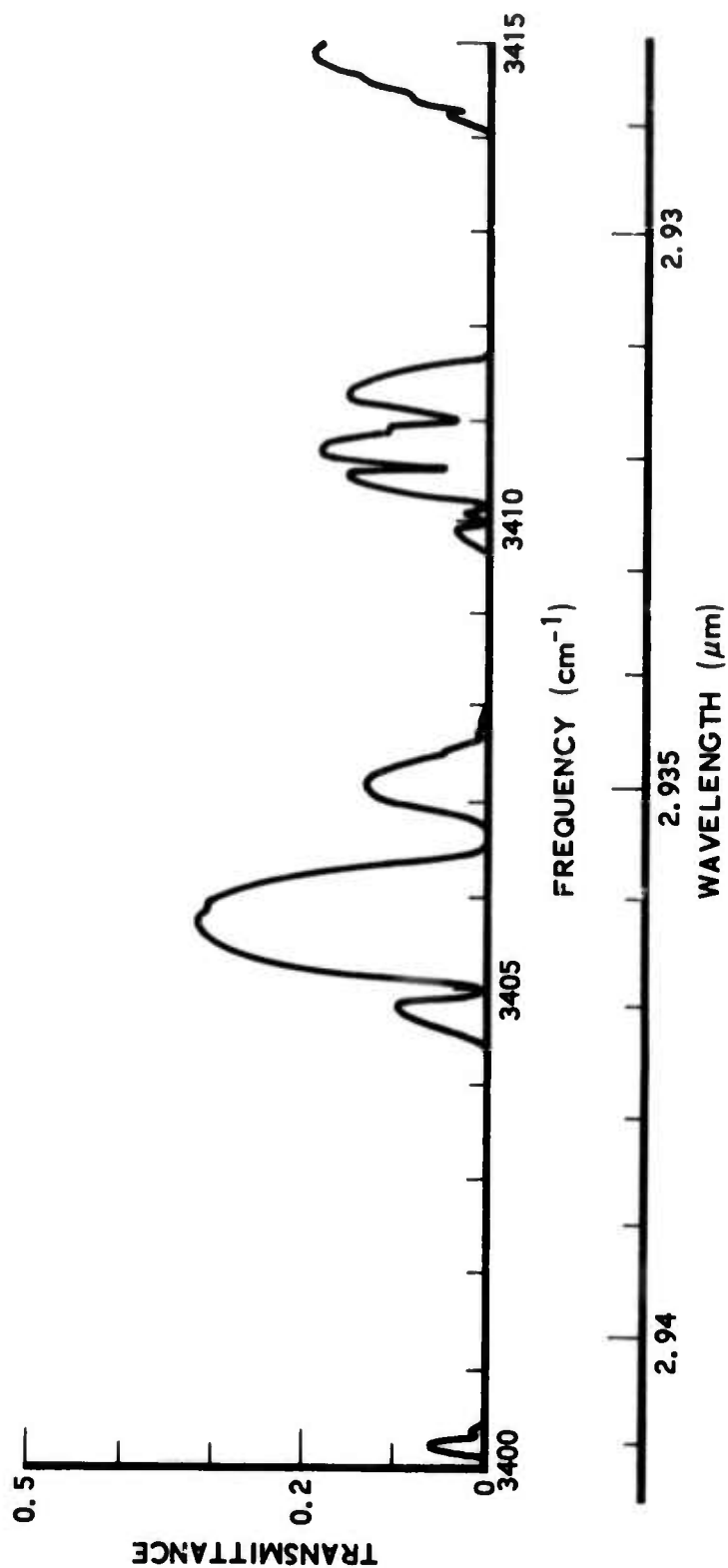


Fig. 5. Transmittance from 0 to 20 km at a 60-Deg Zenith Angle through a Mid-Latitude Summer Atmosphere (The optical path was divided into 40 segments.)

Table 4. Comparison of Segmenting Algorithms for Inhomogeneous Atmosphere

No. of Segments (n)	Equal Geometric Segments			Equal Air Molecule Population Segments		
	\bar{T}_n (3400-3415 cm ⁻¹)	\bar{T}_n / \bar{T}_{40}	Peak (T_n / T_{40})	\bar{T}_n	\bar{T}_n / \bar{T}_{40}	Peak (T_n / T_{40})
40	0.04906	1.0	--	0.04897	1.0	--
20	0.04943	1.0075	1.057	0.04906	1.0018	1.0137
10	0.05084	1.036	1.285	0.04944	1.0096	1.0705
5	0.05686	1.159	2.81	0.05092	1.0398	1.306
2	0.09145	1.864	49.1	0.06356	1.298	5.76
1	0.1360	2.77	291.5	0.1360	2.77	279.5

ratio spectrum shown in Fig. 6, the cross-hatched region indicates where the transmittance was less than 10^{-4} . Peak values in the 15 cm^{-1} band for all the ratio spectra are listed in the columns of Table 4 headed Peak T_n / T_{40} . When the path is divided into 40 segments, the division method makes little difference, but for a more limited number of segments, the equal number of air molecules yields transmittances that are closer to the 40-segment values. For this reason, the equal absorber concentration algorithm has been adopted for the calculations reported later in this discussion. When calculations over inhomogeneous paths are desired, we have chosen, based on the limited data summarized in Table 4, to divide the path into 5 segments. This choice is a compromise between the increased accuracy available with more segments and the increased computation time and cost required to carry out the computations over a broad spectral interval with an increased number of segments.

E. PROGRAM EXECUTION TIME

The time t required for a spectrum computation is directly proportional to the product of the number of segments n_s into which the optical path is divided and the number of spectral values n_v desired plus a small overhead time t_0 required to perform those calculations needed only once per spectrum.

$$t = r n_s n_v + t_0 \quad (12)$$

The rate constant r depends on the density of spectral lines in the spectral region of interest, the breadth of the region of influence included, the speed of the computer, and the efficiency of the program. The INHOM Program described in this report, when operated on the CDC 7600 computer at Aerospace, achieved a rate of $r = 2.2\text{ msec}$ for the spectral region from 3325 to 3975 cm^{-1} and an influence bound of 10 cm^{-1} . Overhead time was

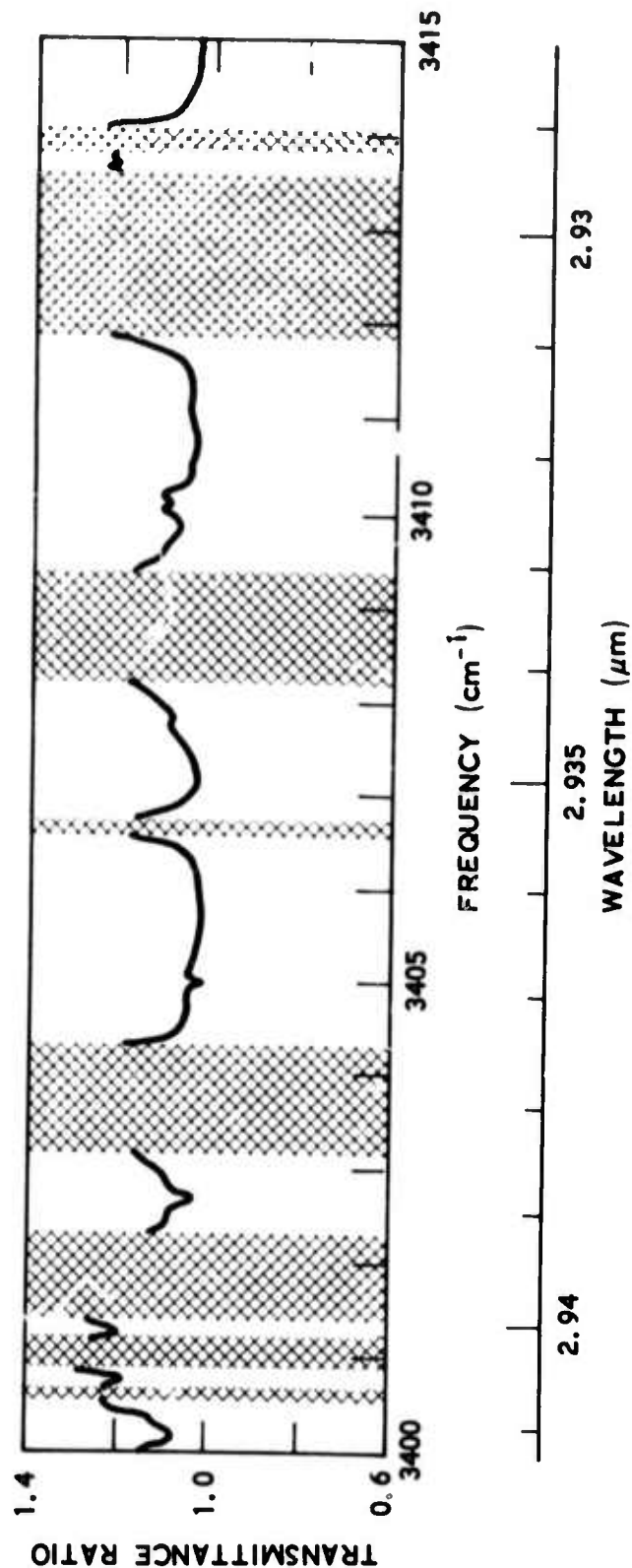


Fig. 6. Ratio of the Transmittance Computed with 5 Segments of Equal Air Molecule Content to the Transmittance Computed with 40 Segments of Equal Air Molecule Content (Crosshatched regions indicate where the transmittance was less than 10^{-4} .)

$t_0 < 1$ sec. The program that achieved this rate included all the pressure-broadening, stimulated-emission, and partition function calculations described previously. The most significant single improvement in speed resulted from coding the computer operations required to implement Eq. (5) in assembly language with an in-line exponential function rather than in FORTRAN. This approach resulted in a 25-percent decrease in r .

III. SOURCE SPECTRAL EFFECTS ON APPARENT ATMOSPHERIC TRANSMITTANCE

A. TEST CASES

Based on initial test cases described in the following paragraphs, errors of up to 79 percent are possible in atmospheric transmittance corrections if source spectral effects are not considered. The initial test source was an isothermal model of the afterburning plume of a typical rocket at 20 km. Characteristics of this target are listed in Table 5.* The plume is assumed to be a right circular cylinder, and an optical path along a diameter of the cylinder has been the only path considered. The radiance was computed at 0.01 cm^{-1} resolution between 3325 and 3975 cm^{-1} . A short segment of the target spectrum is shown in Fig. 7. All corrections discussed in Section II for high temperatures were included, and only emissions from CO_2 and H_2O were considered. No lines other than those listed in the AFCRL atlas were included. This approach leads to an error of unknown magnitude since the AFCRL atlas was developed for atmospheric transmittance work, and bands and lines arising from energy levels that are not appreciably populated at atmospheric temperatures have been omitted from the atlas. Qualitative results indicate that the atlas becomes inadequate for temperatures above about 1000 K. Nevertheless, we have used the atlas to gain a feel for the magnitude of the source spectral effects on atmospheric transmittance, recognizing that quantitative results may not be correct.

Studies have been conducted of the apparent radiance of this source after passing along two different paths through the tropical atmosphere. One is a 100-km horizontal path and the other is a path to space at a 75-deg zenith angle (see Table 6). A transmittance spectrum has been computed for each

* Private communication from D. D. Thomas of the Propulsion Department, Aeroengineering Subdivision, The Aerospace Corporation.

Table 5. Isothermal Typical Target Model

Altitude (km)	Plume Diameter (m)	Plume Length (m)	Temperature (K)	Total Pressure (millibar)	Transverse Path Column Densities (10^{19} mol/cm ²)	
					CO ₂	H ₂ O
1	3.07	20.50	2139.04	897.989	6.432	26.22
5	3.44	37.64	1867.40	553.973	5.090	20.75
10	4.34	71.34	1625.15	278.763	3.716	15.20
15	5.74	133.8	1417.75	129.994	2.628	10.71
20	7.73	237.9	1249.36	59.6024	1.841	7.505
25	10.39	409.5	1107.18	27.6986	1.298	5.292
30	13.79	704.0	957.78	13.1993	0.949	3.869

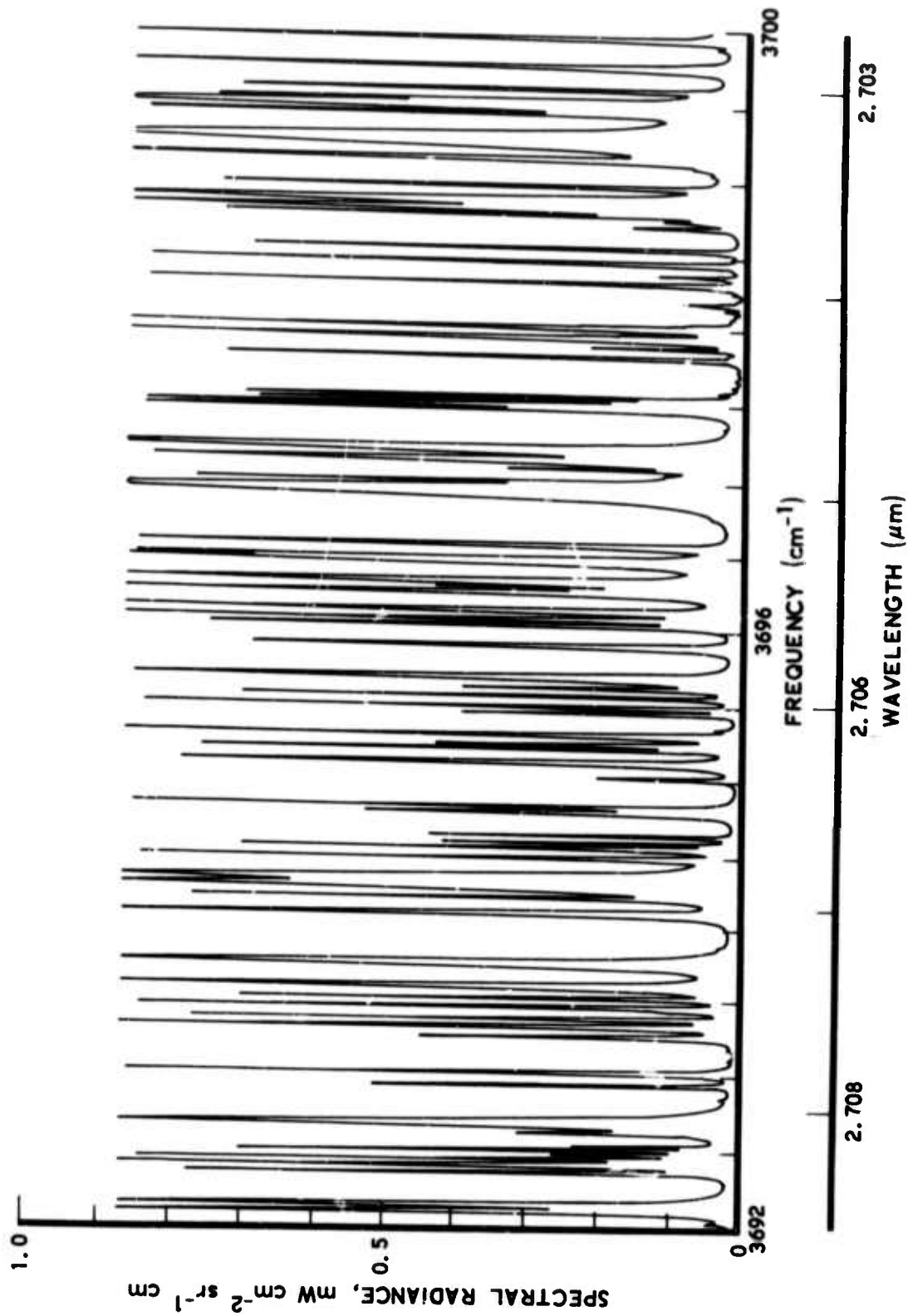


Fig. 7. Radiance from a Typical Target at 20 km Viewed along a Diameter of the Assumed Isothermal Cylindrical Plume

Table 6. Tropical Model Atmosphere⁶

Height (km)	Pressure (mbar)	Temp. (K)	Density (g/m ³)	Water Vapor (g/m ³)	Ozone (g/m ³)
0	1.013E+03	300.0	1.167E+03	1.9E+01	5.6E-05
1	9.040E+02	294.0	1.064E+03	1.3E+01	5.6E-05
2	8.050E+02	288.0	9.689E+02	9.3E+00	5.4E-05
3	7.150E+02	284.0	8.756E+02	4.7E+00	5.1E-05
4	6.330E+02	277.0	7.951E+02	2.2E+00	4.7E-05
5	5.590E+02	270.0	7.199E+02	1.5E+00	4.5E-05
6	4.920E+02	264.0	6.501E+02	8.5E-01	4.3E-05
7	4.320E+02	257.0	5.855E+02	4.7E-01	4.1E-05
8	3.780E+02	250.0	5.258E+02	2.5E-01	3.9E-05
9	3.290E+02	244.0	4.708E+02	1.2E-01	3.9E-05
10	2.860E+02	237.0	4.202E+02	5.0E-02	3.9E-05
11	2.470E+02	230.0	3.740E+02	1.7E-02	4.1E-05
12	2.130E+02	224.0	3.316E+02	6.0E-03	4.3E-05
13	1.820E+02	217.0	2.929E+02	1.8E-03	4.5E-05
14	1.560E+02	210.0	2.578E+02	1.0E-03	4.5E-05
15	1.320E+02	204.0	2.260E+02	7.6E-04	4.7E-05
16	1.110E+02	197.0	1.972E+02	6.4E-04	4.7E-05
17	9.370E+01	195.0	1.676E+02	5.6E-04	6.9E-05
18	7.890E+01	199.0	1.382E+02	5.0E-04	9.0E-05
19	6.660E+01	203.0	1.145E+02	4.9E-04	1.4E-04
20	5.650E+01	207.0	9.515E+01	4.5E-04	1.9E-04
21	4.800E+01	211.0	7.938E+01	5.1E-04	2.4E-04
22	4.090E+01	215.0	6.645E+01	5.1E-04	2.8E-04
23	3.500E+01	217.0	5.618E+01	5.4E-04	3.2E-04
24	3.000E+01	219.0	4.763E+01	6.0E-04	3.4E-04
25	2.570E+01	221.0	4.045E+01	6.7E-04	3.4E-04
30	1.220E+01	232.0	1.831E+01	3.6E-04	2.4E-04
35	6.000E+00	243.0	8.600E+00	1.1E-04	9.2E-05
40	3.050E+00	254.0	4.181E+00	4.3E-05	4.1E-05
45	1.590E+00	265.0	2.097E+00	1.9E-05	1.3E-05
50	8.540E-01	270.0	1.101E+00	6.3E-06	4.3E-06
70	5.790E-02	219.0	9.210E-02	1.4E-07	8.6E-08
100	3.000E-04	210.0	5.000E-04	1.0E-09	4.3E-11

⁶R. A. McClatchey, R. W. Fenn, J. E. A. Selby, F. E. Volz, and J. S. Garing, Optical Properties of the Atmosphere (Third Ed.), Environmental Research Paper No. 411, AFCRL-72-0497, Air Force Cambridge Research Laboratories, Mass. (24 August 1972).

of these paths at 0.01 cm^{-1} resolution from 3325 to 3975 cm^{-1} . A sample segment of such a spectrum is illustrated in Fig. 8. In addition, an apparent radiance spectrum has been obtained for each of these paths by multiplying the transmittance spectrum for the path by the source radiance function. A sample segment of such an apparent radiance spectrum for the 75-deg , zenith angle slant path is shown in Fig. 9.

B. ATMOSPHERIC TRANSMITTANCE EFFECTIVE FOR LOW RESOLUTION SENSOR

A variety of atmospheric transmittance values can be obtained from the spectra presented in paragraph III. A when a sensor with a spectral bandwidth greater than a few line widths is considered. The differences depend on the way in which the low spectral resolution transmittance is defined.

The effective average transmittance \bar{T}_e is the applicable value if the objective of sensor measurements is the inference of the source radiance.

$$\bar{T}_e = \frac{\int_{\nu_1}^{\nu_2} L_a(\nu) d\nu}{\int_{\nu_1}^{\nu_2} L_t(\nu) d\nu} = \frac{\int_{\nu_1}^{\nu_2} L_t(\nu) T(\nu) d\nu}{\int_{\nu_1}^{\nu_2} L_t(\nu) d\nu} \quad (13)$$

is the ratio of the integrated apparent radiance $L_a(\nu)$ to the integrated target radiance $L_t(\nu)$. Spectra of \bar{T}_e for the two optical paths considered are indicated by solid lines in Figs. 10 and 11. The value $\Delta\nu = \nu_2 - \nu_1 = 20 \text{ cm}^{-1}$ was used in computing these spectra. Three values of \bar{T}_e obtained for bandwidths greater than 20 cm^{-1} in the two wings and the center of the absorption region shown in Figs. 10 and 11 are listed in Table 7. The entry in Table 7 titled " 20 cm^{-1} Intermediate Average" is the average of the \bar{T}_e curve from Fig. 10 or 11 for the same radiometer bandwidth. This indicates that the average of low resolution spectra does not produce the same results as the average obtained from high resolution spectra.

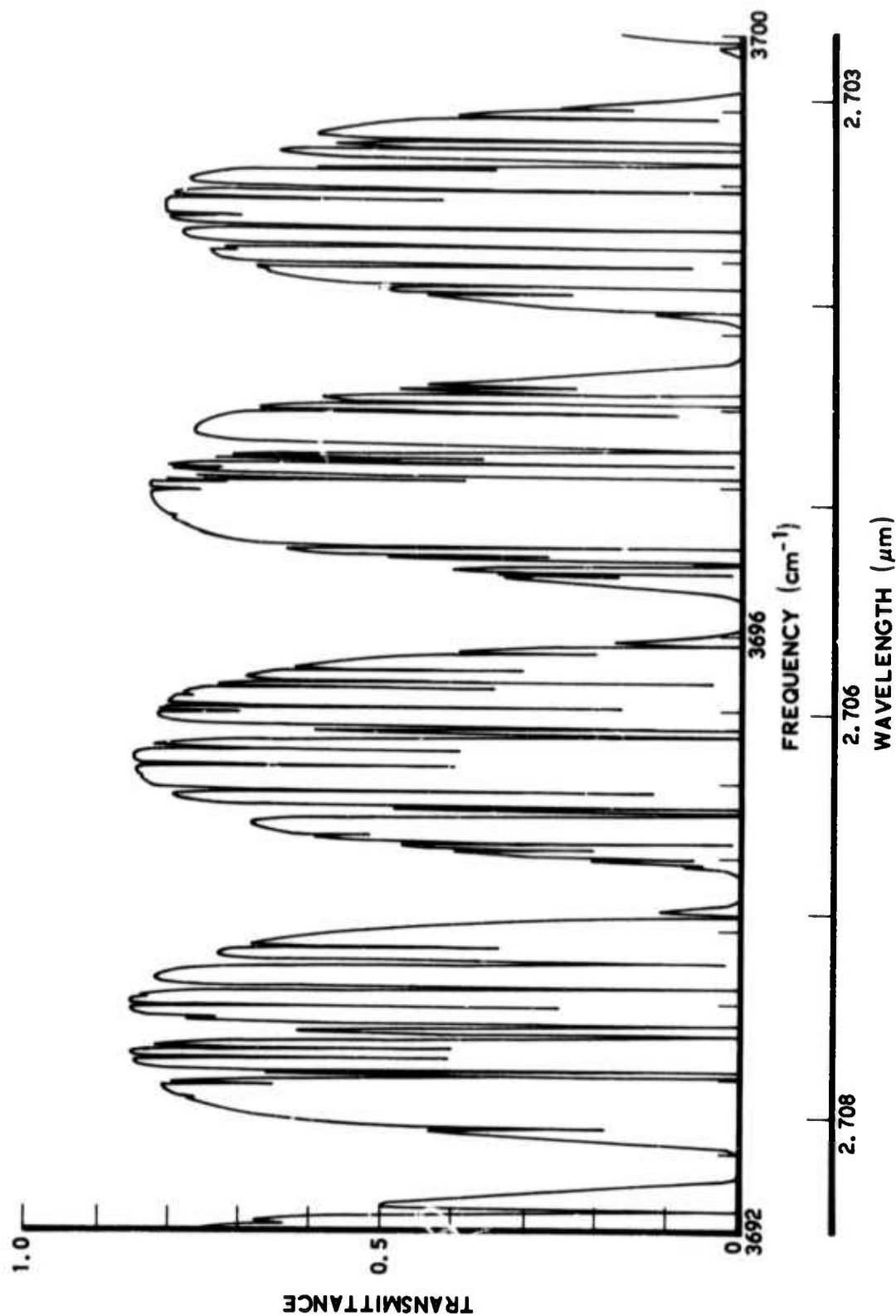


Fig. 8. Transmittance of the Atmosphere along a Path from 20 km to Space at a 75-Deg Zenith Angle through a Tropical Atmosphere

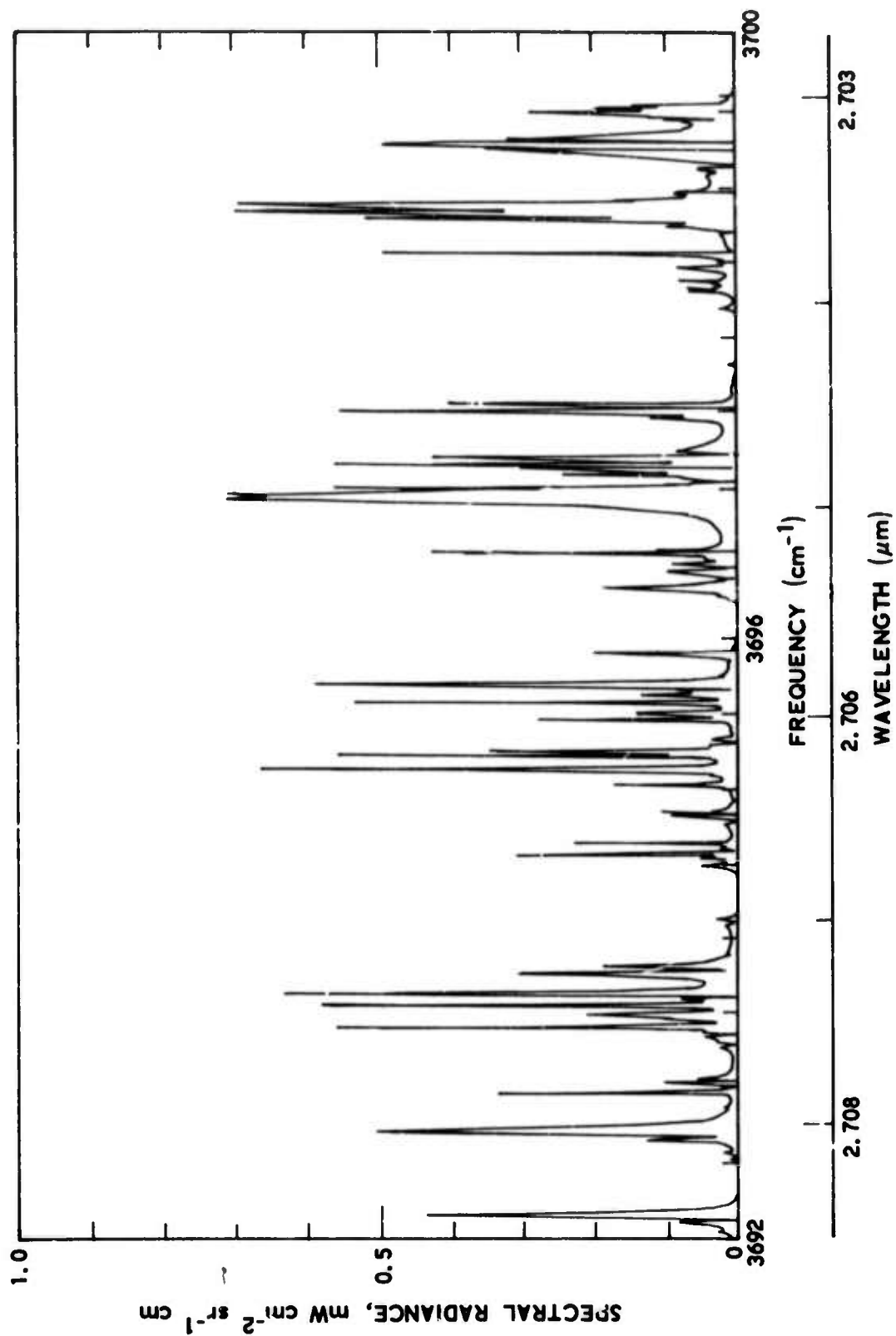


Fig. 9. Apparent Spectral Radiance of a Typical Target after Traversing a Path through the Atmosphere from 20 km to Space at a 75-Deg Zenith Angle

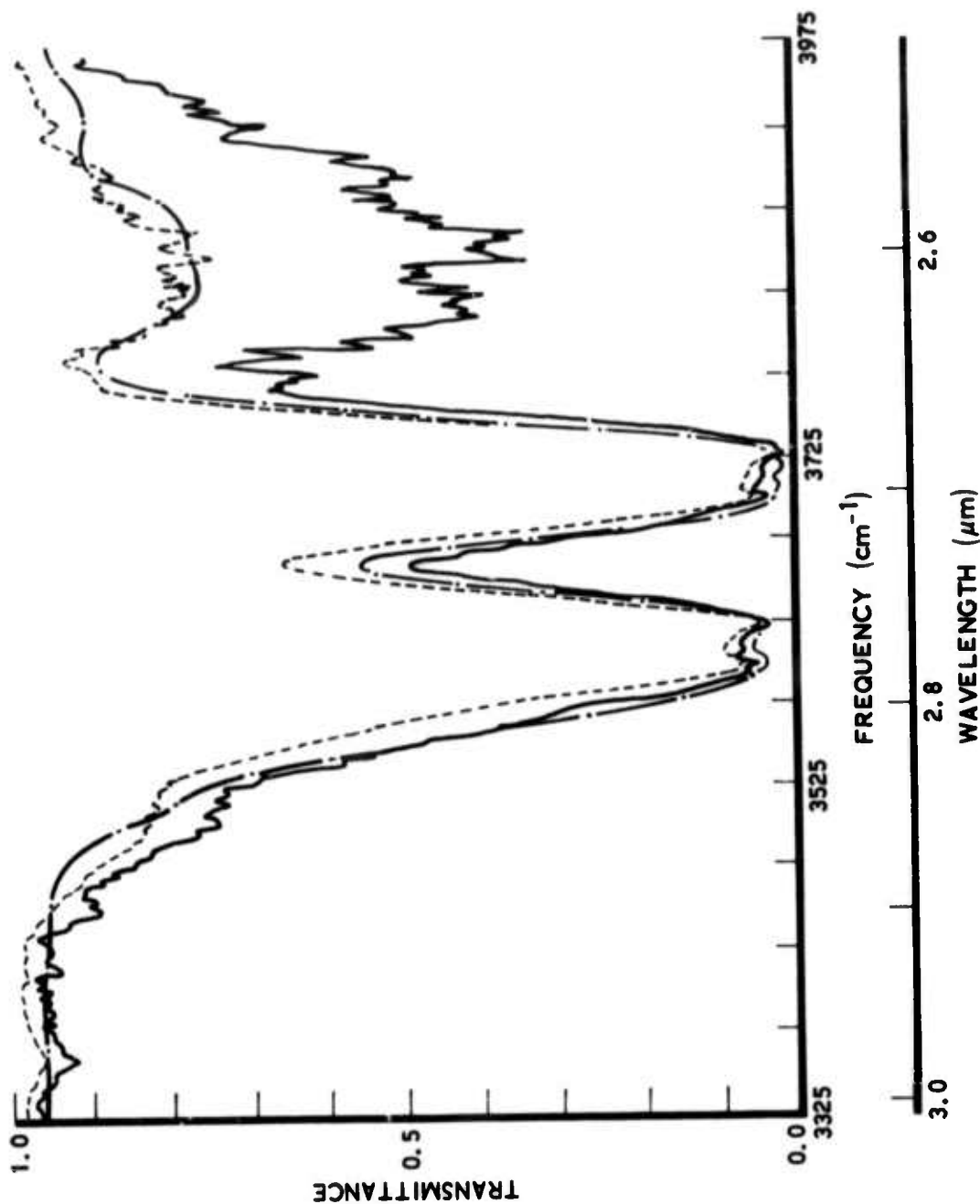


Fig. 10. Transmittance Computed in Several Ways for a Horizontal Path 100 km Long at 20 km Altitude (The solid curve — is the effective average transmittance for a typical missile plume. The dashed curve --- is the average transmittance. The dash-dot curve - · - · - is the average transmittance obtained from high resolution calculations averaged over 20 cm⁻¹. The - - - curve is the approximation to the average transmittance provided by the AFCRL LOWTRAN computer program.)

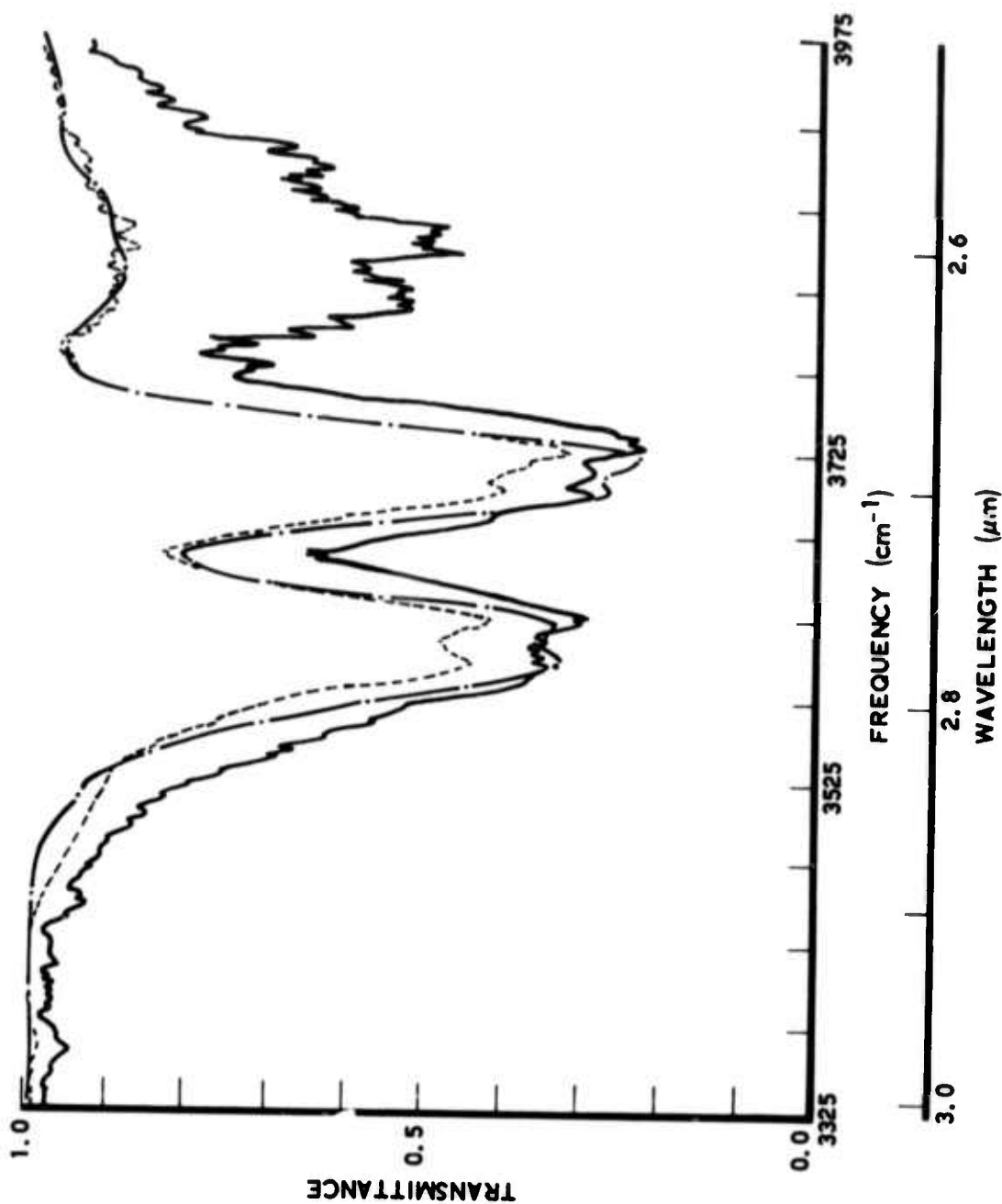


Fig. 11. Transmittance Computed in Several Ways for a Slant Path from 20 km to Space at a 75-Deg Zenith Angle (The solid curve — is the effective average transmittance for a typical missile target. The dashed curve - - - - is the average transmittance. These two curves were obtained from high resolution calculations. The - · - · curve is the approximation to the average transmittance provided by the AFCRL LOWTRAN code.)

Table 7. Radiometer Transmittance

Path:	20 km to Space, 75-Deg Zenith Angle						100-km Horizontal at 20 km					
	3350 - 3575		3575 - 3725		3725 - 3950		3350 - 3575		3575 - 3725		3725 - 3950	
Band Limits (cm^{-1})	Trans.	% Diff.	Trans.	% Diff.	Trans.	% Diff.	Trans.	% Diff.	Trans.	% Diff.	Trans.	% Diff.
Effective Average, \bar{T}_e	0.8303	---	0.3971	---	0.5608	---	0.7508	---	0.1561	---	0.4337	---
20 cm^{-1} , Intermediate Av.	0.8661	4.3	0.4033	1.6	0.6119	9.11	0.8020	6.8	0.1631	4.5	0.4954	14.2
ATLES Estimate, \bar{T}_{eb}	0.7534	-9.3	0.2745	-30.9	0.4321	-22.9	0.6324	-15.8	0.09103	-48.1	0.2602	-40.0
Average, \bar{T}	0.9325	12.3	0.5579	40.5	0.8707	55.3	0.8658	15.3	0.2375	52.1	0.7756	78.8
LOWTRAN, Estimate	0.9351	12.6	0.4683	17.9	0.8652	54.3	0.8329	10.9	0.1714	9.8	0.7429	71.3
ATLES, Estimate	0.9377	12.9	0.5832	46.9	0.8704	55.2	0.8666	15.4	0.2695	72.6	0.7693	77.4
Low Resolu- tion Effect. Average, T_{eL}	0.9119	9.8	0.5508	38.7	0.8081	44.1	0.8262	10.0	0.2290	46.7	0.6818	57.2

The average transmittance \bar{T} is the most frequently computed or approximated transmittance.

$$\bar{T} = \frac{1}{\Delta\nu} \int_{\nu_1}^{\nu_2} T(\nu) d\nu \quad (14)$$

The average transmittance for the two sample paths was computed from the high resolution transmittance spectra by averaging over $\Delta\nu = 20 \text{ cm}^{-1}$. Results are indicated by dashed curves in Figs. 10 and 11. Average transmittances for wider bands are shown in Table 7. For sources of uniform spectral radiance, \bar{T} should be the same as \bar{T}_e , but for line sources such as hot gases, they are clearly not the same.

The factor \bar{T} is the quantity approximated by most atmospheric transmittance band model procedures. Estimates of \bar{T} by two such programs for the two sample paths are included for comparison in Table 7. In the table, LOWTRAN refers to the program developed by R. A. McClatchey at the Air Force Cambridge Research Laboratories,^{6,7} and ATLES refers to a band model developed at Aerospace to account for source effects.¹ Spectra computed with the use of LOWTRAN are indicated by the broken curves in Figs. 10 and 11. The comparisons given in Table 7 indicate that the band models approximate \bar{T} reasonably well. The discrepancy between the \bar{T} spectrum and the LOWTRAN estimate for the 75-deg slant path is not understood at present.

An attempt to include source effects can be made by using low resolution source and transmittance functions to compute low resolution effective transmittance \bar{T}_{eL} .

⁷ J. E. A. Selby and R. A. McClatchey, Atmospheric Transmittance from 0.25 to 28.5 μm : Computer Code LOWTRAN2, Environmental Research Paper No. 427, AFCRL-72-0745, Air Force Cambridge Research Laboratories, Mass. (29 December 1972).

$$\bar{T}_{eL} = \frac{\sum_i T(\Delta\nu_i) L_t(\Delta\nu_i)}{\sum_i L_t(\Delta\nu_i)} \quad (15)$$

The results of carrying this out for the wings and center of the 2.7- μ m absorption are given in Table 7. The accuracy of estimating \bar{T}_e in this way is only a little better than the average transmittance \bar{T} obtained without considering the source spectrum in any way.

The techniques of band modeling can be applied directly to the definition of the effective average transmittance, Eq. (13), to obtain \bar{T}_{eB} . These procedures are discussed in detail in Ref. 1, as are spectral comparisons of the effective average transmittances derived from the band model and from high resolution calculations. Included in Table 7 is the radiometer transmittance predicted by this special band model, which is the only procedure that explicitly takes into account line-correlation relations between the source and atmosphere in estimating \bar{T}_e . It is also the only procedure that does not overestimate the transmittance. In fact, if any conclusions may possibly be drawn about the band model from this limited set of data, it would appear that the model overestimates the effects of line correlation.

Based on the limited test cases presented in this discussion, one may conclude that all average transmittance procedures, which do not account for possible line correlations, tend to overestimate the effective transmittance of the atmosphere for a line source. In some spectral regions and over some atmospheric paths, this can lead to errors of up to 79 percent in the estimated effective transmittance.

IV. PROGRAM AND LINE ATLAS EVALUATION

A. COMPARISON OF COMPUTED SPECTRA AND EXPERIMENTAL RESULTS

A comparison of computed and experimentally determined spectra has been made for a limited number of cases to demonstrate the overall accuracy of the high resolution computation procedures outlined when they are applied with the AFCRL line atlas. Only H_2O and CO_2 have been studied as they are the principal atmospheric absorbers and source emitters in the spectral region of interest in the present study. Four experimental spectra were chosen, two characteristic of atmospheric paths and two somewhat characteristic of missile plumes. The conditions for each case are listed in Table 8, and the spectra are illustrated in Figs. 12 through 16. Experimental spectra are indicated by solid lines and calculated spectra by dashed lines in the figures.

B. ATMOSPHERIC CO_2 PATH

Experimental CO_2 spectra characteristic of atmospheric paths have been obtained from the work of Burch,⁸ and his Sample 10 has been chosen for detailed comparison. A low resolution spectrum for this sample, illustrated in Fig. 12 by a solid line, was obtained by differentiating the integrated absorption spectrum tabulated in Ref. 8 and converting the result to a transmittance spectrum. The computed comparison spectrum (dashed line in Fig. 12) was derived by convolving a high resolution spectrum obtained by means of the INHOM Program from the AFCRL line atlas with a 2.5 cm^{-1} full width at half maximum (FWHM) triangular instrument function. Except in the region from about 3660 to 3725 cm^{-1} , agreement of the calculated and

⁸D. E. Burch, D. A. Gryvnak, and R. R. Patty, Absorption by CO_2 Between 3100 and 4100 cm^{-1} (2.44 - 3.22 Microns), U-4132, Aeronutronic Division of Philco-Ford, Newport Beach, California (30 April 1968).

Table 8. Conditions for Experimental Comparison with Computed Spectra

Absorber	CO ₂	H ₂ O	CO ₂	H ₂ O
Absorber Partial Pressure, mb	7.731	9.798	2026.5	949.8
Total Pressure, mb	3	963.6	2026.5	949.8
Temperature, K	296	296	1146	1040
Path Length, m	237	121	0.60	0.60
Column Density, 1020 mol/cm ²	44.835	29.011	7.6849	3.9689
Reference	Sample 10 of Ref. 8	Sample 39 of Ref. 9	Fig. 6 of Ref. 10	Fig. 47 of Ref. 11

⁹D. E. Burch, D. A. Gryvnak, and R. R. Patty, Absorption by H₂O Between 2800 and 4500 cm⁻¹ (2.7 Micron Region), U-3202, Aeronutronic Division of Philco-Ford, Newport Beach, California (30 September 1965).

¹⁰F. S. Simmons, H. Y. Yamada, and C. B. Arnold, Measurements of Temperature Profiles in Hot Gases by Emission-Absorption Spectroscopy, University of Michigan Report WRL 8962-18-F, NASA CR-72491, Willow Run Laboratories (April 1969).

¹¹F. S. Simmons, C. B. Arnold, and D. H. Smith, Studies of Infrared Radiative Transfer in Hot Gases 1: Spectral Absorbance Measurements in the 2.7 μ H₂O Bands, University of Michigan Report 4613-91-T, Willow Run Laboratories (August 1965).

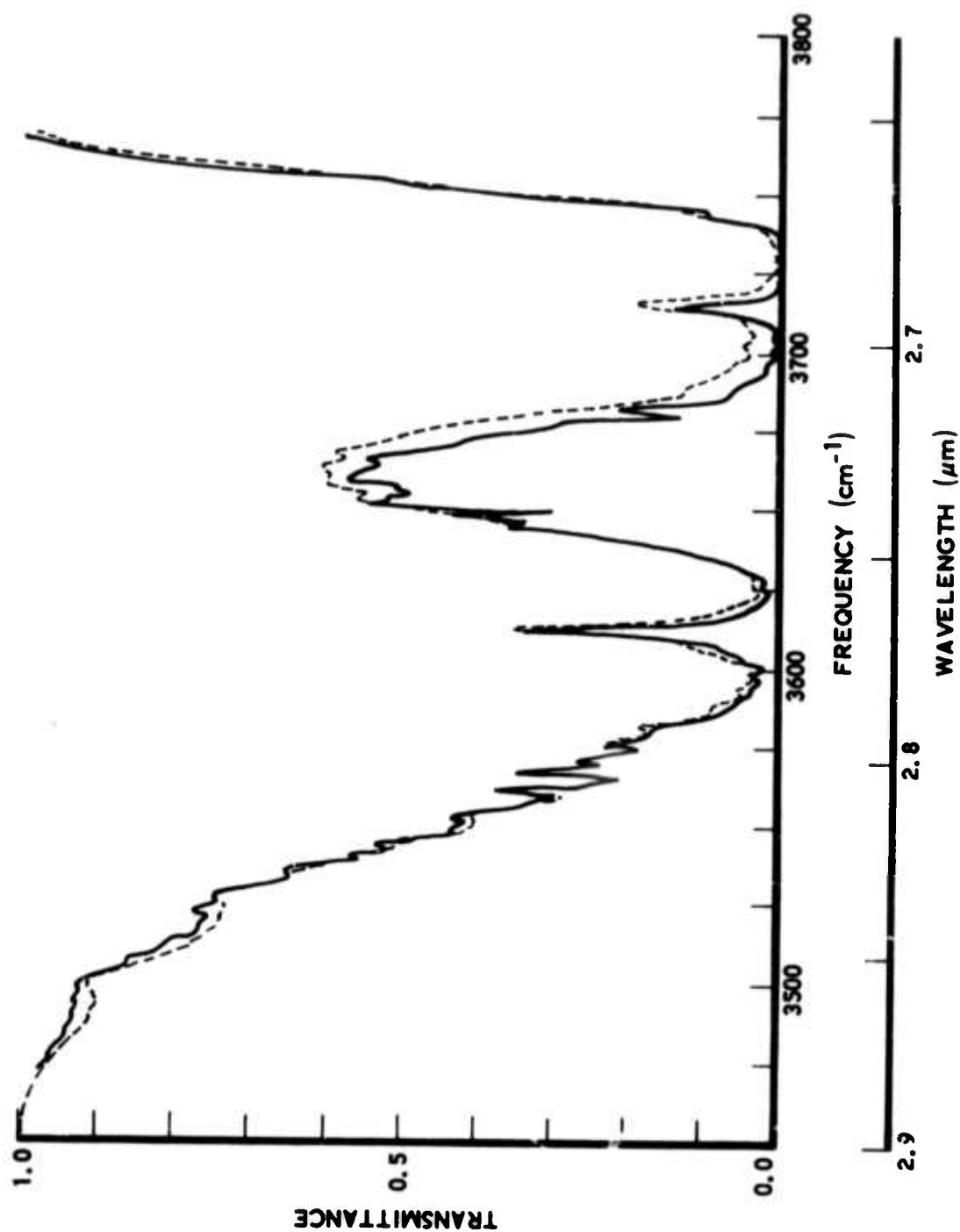


Fig. 12. Comparison of Computed CO₂ Transmittance with Low Resolution Experimental Observations Characteristic of Atmospheric Paths (The conditions are listed in Table 8. The solid curve was obtained from the absorption tabulation in Ref. 8. The dashed curve was obtained from the AFCRL atlas of spectroscopic parameters by the means outlined in the text for the experimental conditions listed in Table 8.)

experimental values is good. In the region where agreement is less satisfactory, the apparent disagreement may be the result of the procedures employed to obtain the spectrum plotted as the experimental spectrum. However, the high resolution comparison made for these same experimental conditions, discussed in the following paragraphs, indicates there is a real difference between the calculated and experimental values in this spectral region.

Figure 13 is a higher resolution spectrum for the same CO_2 sample of Dorch.⁸ The experimental spectrum was obtained in this case by photographing the spectrum in Ref. 8, enlarging it, and then using an "OSCAR" digitizing machine to punch on cards the x and y-coordinates of minima, maxima, and inflection points that characterize the spectrum. These cards containing x and y coordinates then became input data to a computer program to produce the linear wave number plot indicated by the solid curve in Fig. 13. When the initial computer-generated plot of the experimental data was compared with the plot of the calculated spectrum, there appeared to be a constant shift of major spectral features, though the major features seemed to be the correct distance apart spectrally. Since the entire experimental frequency scale depends on the accuracy of the location of two tick marks placed on the original spectrum in Ref. 8, we felt justified in slipping the experimental spectra in frequency space until the major features agreed in location with the calculated features. This required a shift of less than 1 cm^{-1} . Nevertheless, for this reason absolute frequency comparisons are not possible from Fig. 13. The detailed shape of individual spectral features may also be distorted slightly in Fig. 13 because of finite sampling of the spectrum in the digitization process. The computed spectrum indicated by the dashed line was obtained by convolving a triangular instrument function 0.8 cm^{-1} wide (FWHM) with the high resolution spectrum obtained for the experimental conditions from the AFCRL line atlas by means of the INHOM computer program.

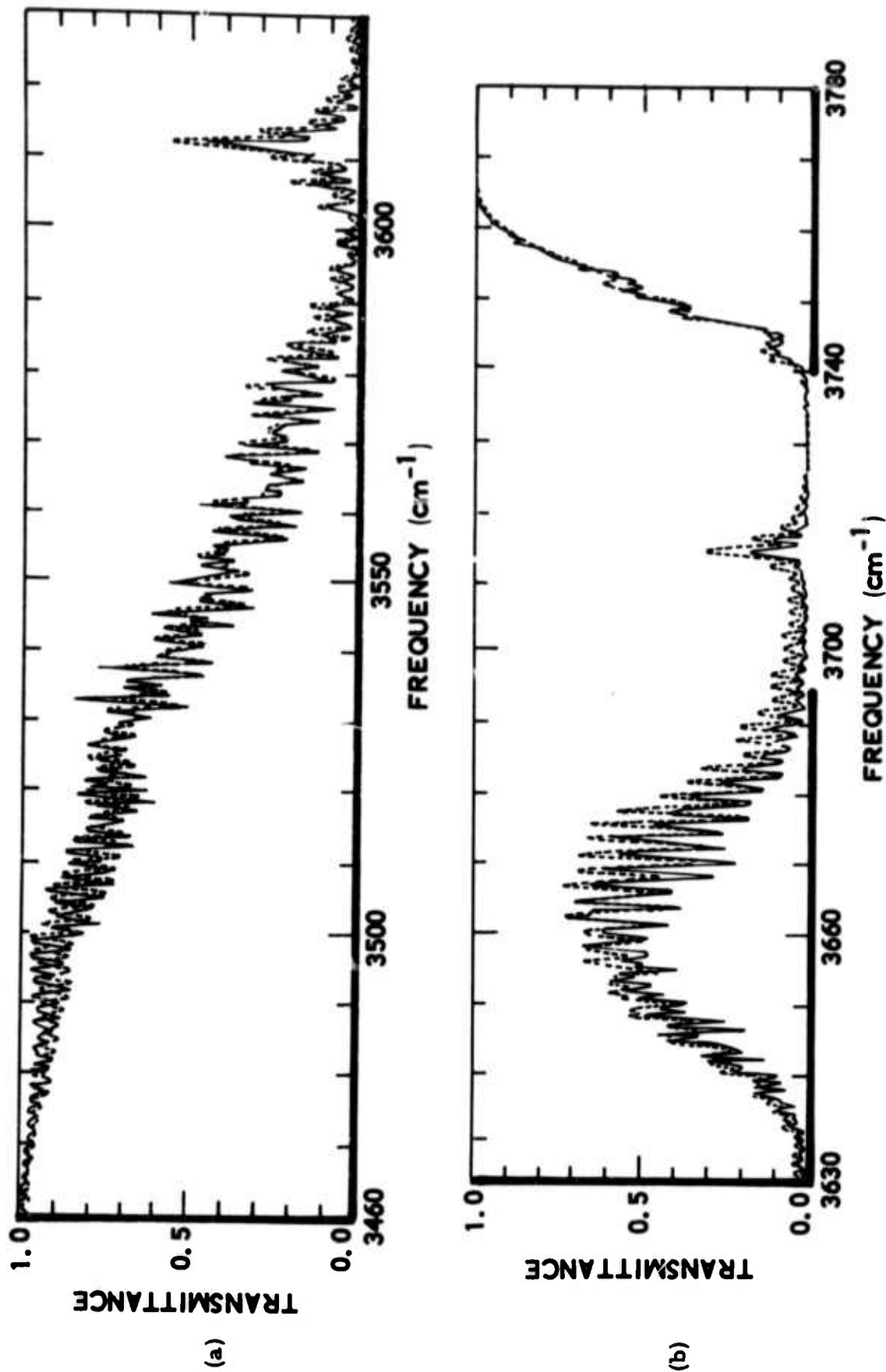


Fig. 13. Comparison of Computed CO_2 Transmittance with High Resolution Laboratory Experimental Observations Characteristic of Atmospheric Paths (The conditions are listed in Table 8. The solid curve was obtained from the spectrum published in Ref. 8 by means discussed in the text. The dashed curve was calculated from the AFCRL atlas of spectroscopic parameters by means of the computer programs discussed in this report.)

Based on the CO₂ spectra for a single sample presented here, the AFCRL line atlas and INHOM Program appear capable of predicting with adequate accuracy the absorption of CO₂ in the 2.7-μm spectral region for typical terrestrial atmospheric conditions. Agreement between the computed and experimental spectra in Fig. 13 is good except in the region from 3660 to 3720 cm⁻¹, where the computed transmittance is somewhat higher than the experimental transmittance, and below about 3520 cm⁻¹, where the positions of various features do not seem to agree very well. The difference between 3660 and 3720 cm⁻¹ is probably real, while the low wave number difference is probably uncorrected scale shift in our reproduction of the original data and is probably not real.

C. ATMOSPHERIC H₂O PATH

Figure 14 is a high resolution spectrum of water obtained by Burch⁹ and identified as Sample 39. The experimental transmittance spectrum was tabulated in Ref. 9, and thus no reproduction scale changes or interpolations have been required. The computed spectrum shown by the dashed curve in Fig. 14 was obtained by convolving the triangular instrument function 0.5 cm⁻¹ wide (FWHM) with the high resolution spectrum obtained from the AFCRL line atlas by means of the INHOM computer program, which employed the experimental conditions listed in Table 8.

Throughout most of the spectrum, agreement between computed and experimental values is good. However, at the low wave number end of the spectrum, there are a number of spectral features in the computed spectrum that do not appear in the experimental spectrum. These have been traced to an error in the AFCRL line atlas. In Fig. 14(a), the relative strengths appearing in the AFCRL line atlas for the strong lines, belonging to the 010 to 030 band, that lie between 2930 and 3000 cm⁻¹ have been represented by vertical lines. There is a very good correlation between the position of these lines and the extra features in the computed spectrum. The strength of this band has been approximated by summing the strengths of all lines

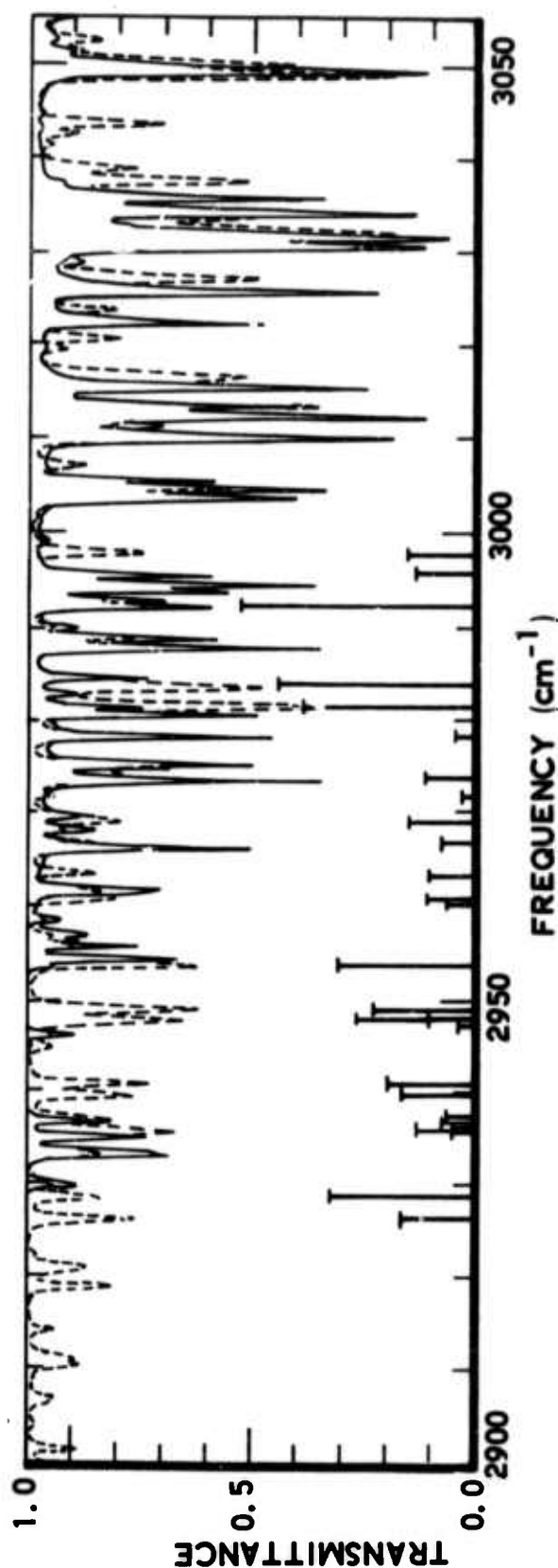


Fig. 14(a). Comparison of Computed H_2O Transmittance with High Resolution Laboratory Experimental Observations Characteristic of Atmospheric Paths (The conditions are listed in Table 8. The solid curve was obtained from the tabulation of experimental data in Ref. 9, and the dashed curve was calculated from the AFCRL atlas of spectroscopic parameters with the use of computer programs discussed in this report. Vertical lines represent the relative strengths of the lines belonging to the Q_{30} to Q_{10} band of water that lie in the spectral region from 2925 cm^{-1} to 3000 cm^{-1} . These lines help to identify the extraneous features in the calculated spectrum.)

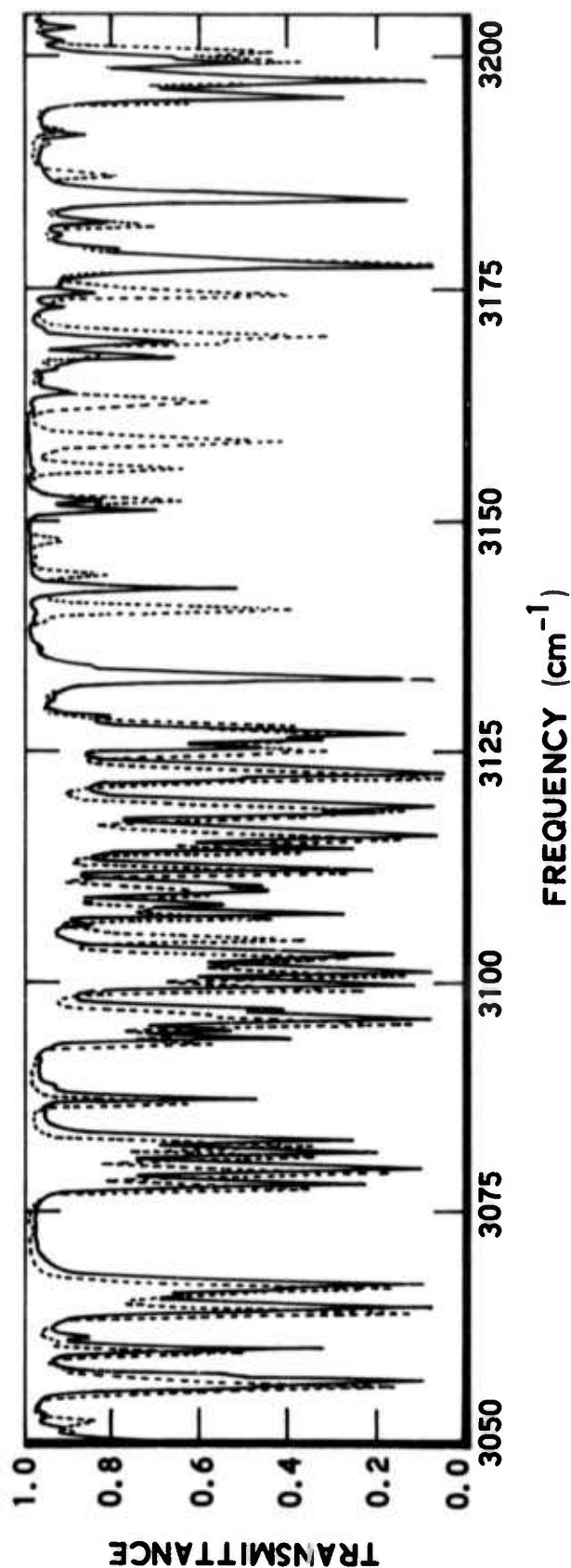


Fig. 14(b). Comparison of Computed H_2O Transmittance with High Resolution Laboratory Experimental Observations Characteristic of Atmospheric Paths (The conditions are listed in Table 8. The solid curve was obtained from the tabulation of experimental data in Ref. 9, and the dashed curve was calculated from the AFCRL atlas of spectroscopic parameters with the use of computer programs discussed in this report.)

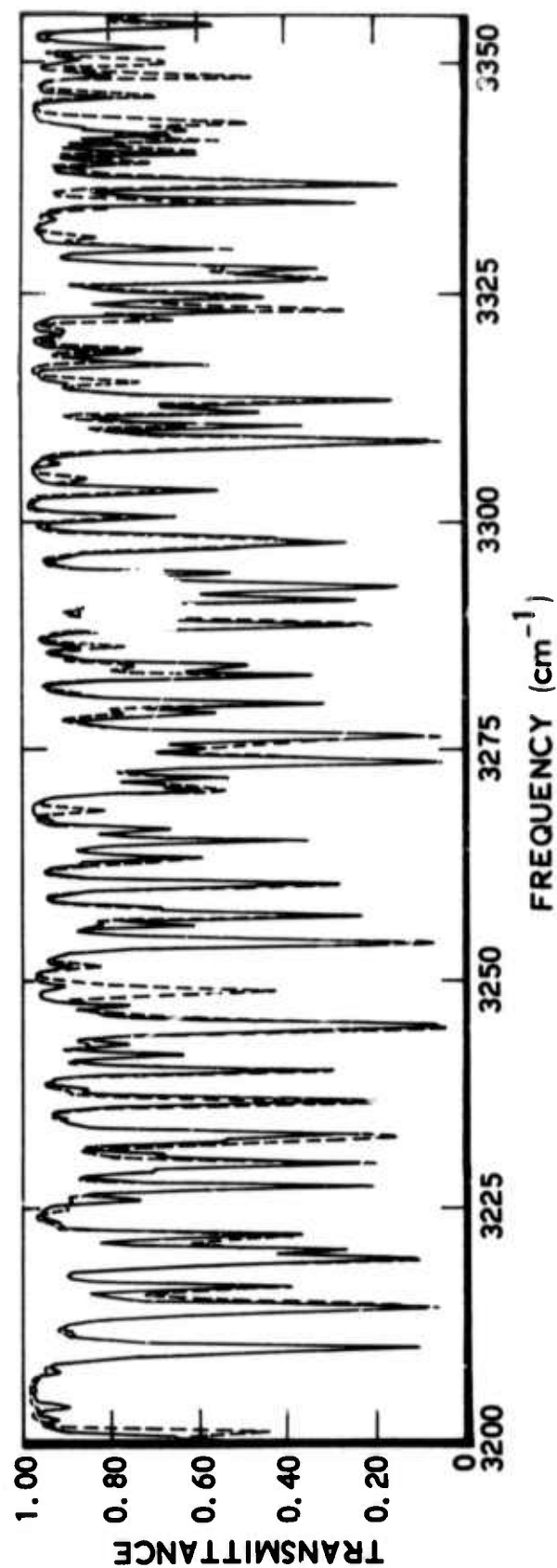


Fig. 14(c). Comparison of Computed H_2O Transmittance with High Resolution Laboratory Experimental Observations Characteristic of Atmospheric Paths (The conditions are listed in Table 8. The solid curve was obtained from the tabulation of experimental data in Ref. 9, and the dashed curve was calculated from the AFCRL atlas of spectroscopic parameters with the use of computer programs discussed in this report.)

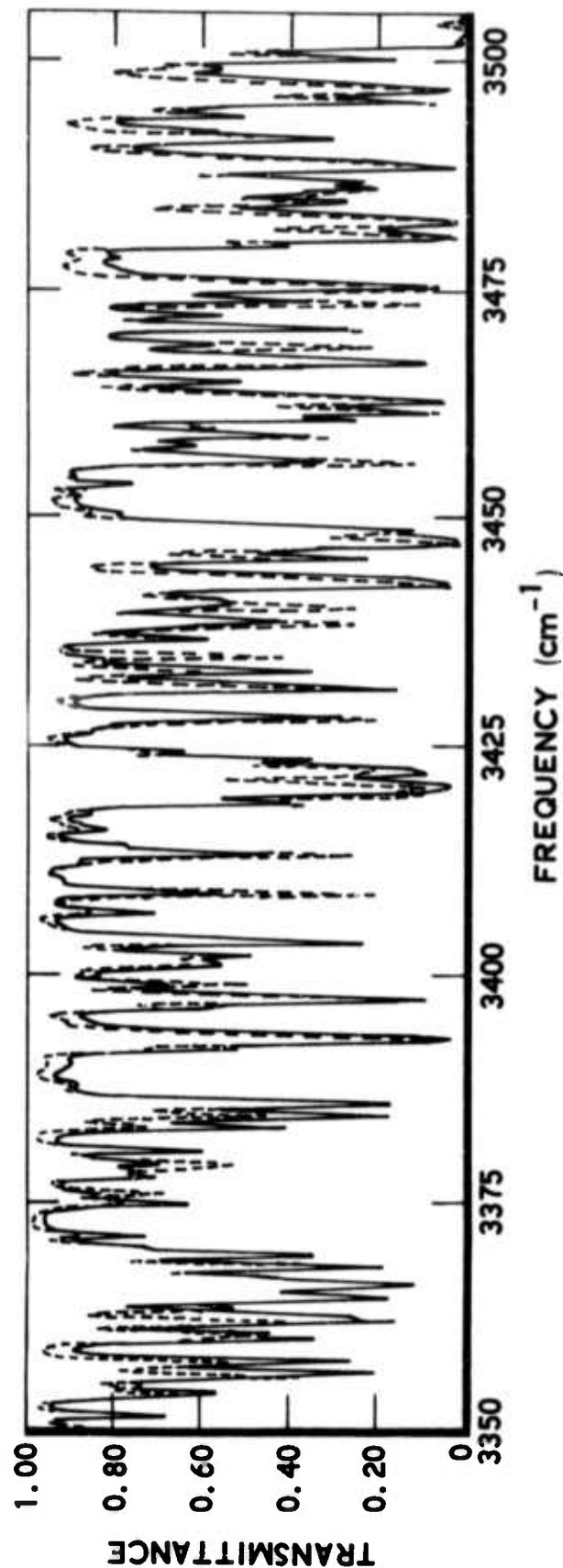


Fig. 14(d). Comparison of Computed H_2O Transmittance with High Resolution Laboratory Experimental Observations Characteristic of Atmospheric Paths (The conditions are listed in Table 8. The solid curve was obtained from the tabulation of experimental data in Ref. 9, and the dashed curve was calculated from the AFCLR atlas spectroscopic parameters with the use of computer programs discussed in this report.)

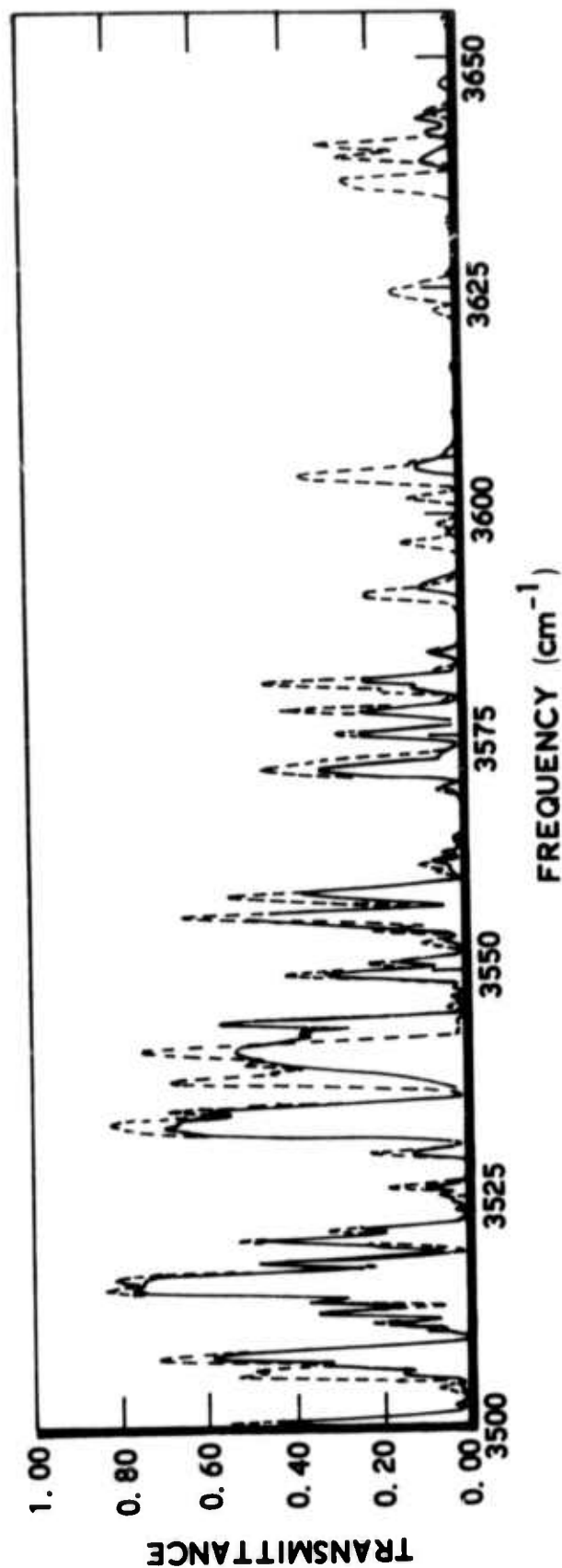


Fig. 14(e). Comparison of Computed H_2O Transmittance with High Resolution Laboratory Experimental Observations Characteristic of Atmospheric Paths (The conditions are listed in Table 8. The solid curve was obtained from the tabulation of experimental data in Ref. 9, and the dashed curve was calculated from the AFCRL atlas of spectroscopic parameters with the use of computer programs discussed in this report.)

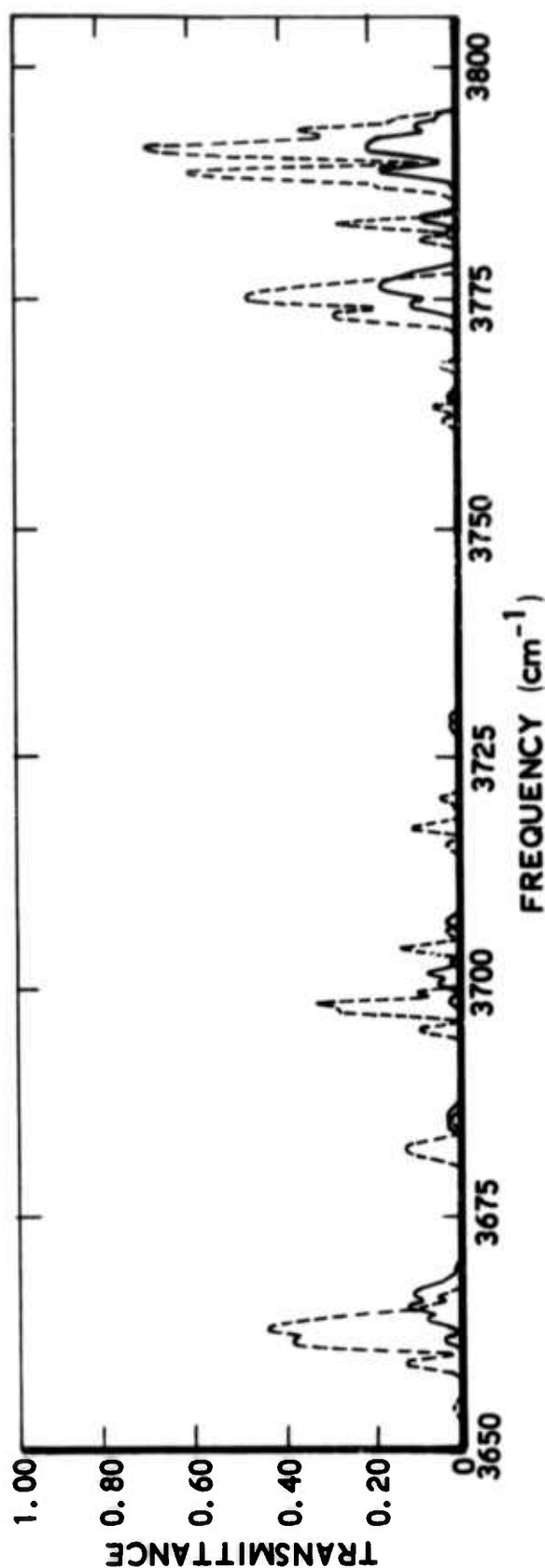


Fig. 14(f). Comparison of Computed H_2O Transmittance with High Resolution Laboratory Experimental Observations Characteristic of Atmospheric Paths (The conditions are listed in Table 8. The solid curve was obtained from the tabulation of experimental data in Ref. 9, and the dashed curve was calculated from the AFCRL atlas of spectroscopic parameters with the use of computer programs discussed in this report.)

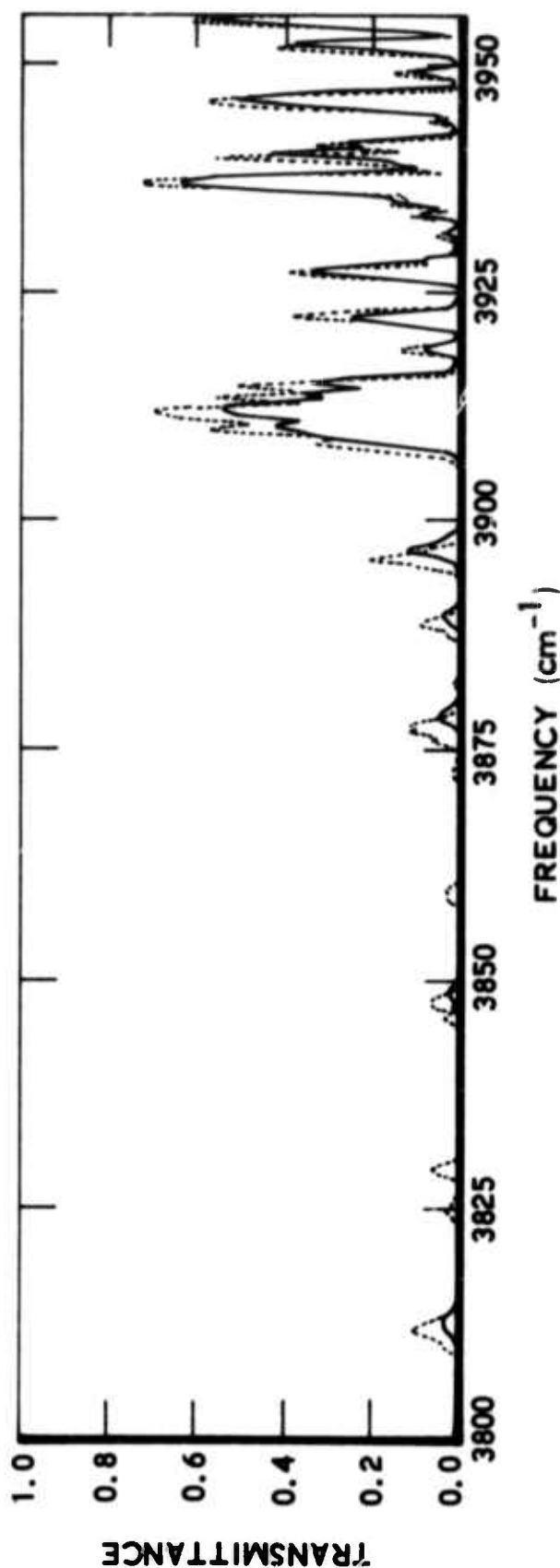


Fig. 14(g). Comparison of Computed H₂O Transmittance with High Resolution Laboratory Experimental Observations Characteristic of Atmospheric Paths (The conditions are listed in Table 8. The solid curve was obtained from the tabulation of experimental data in Ref. 9, and the dashed curve was calculated from the AFCRL atlas of spectroscopic parameters with the use of computer programs discussed in this report.)

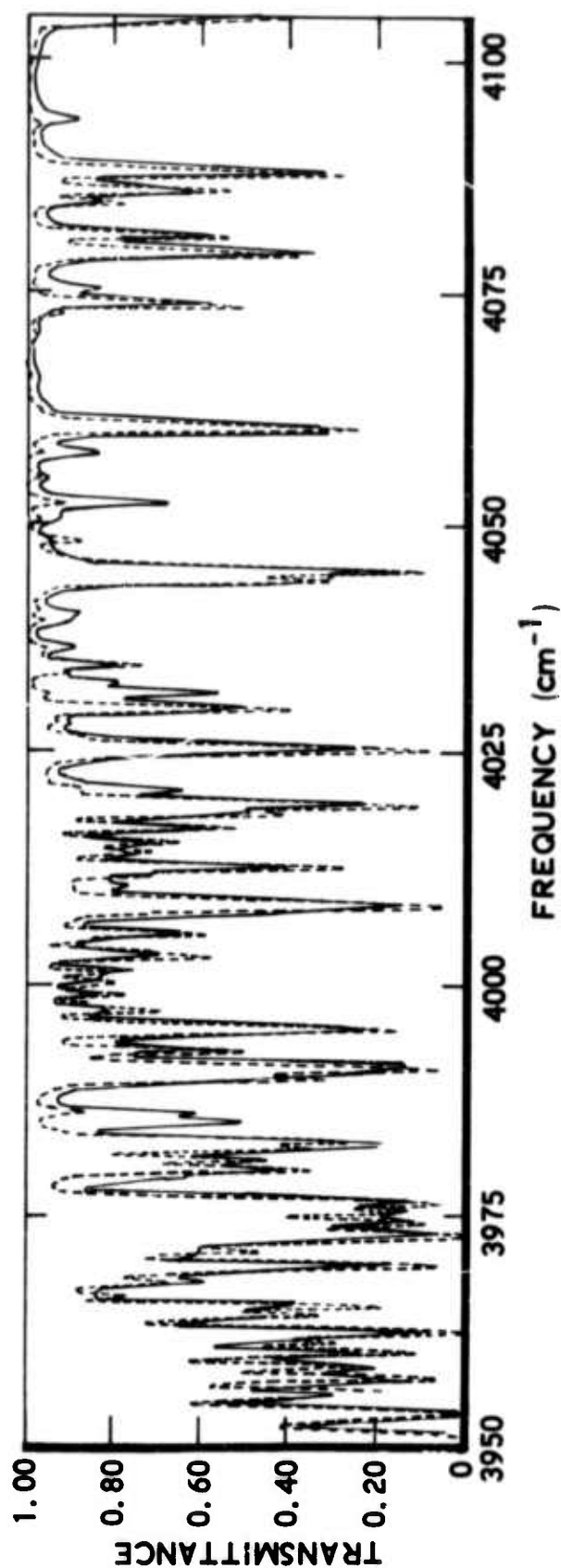


Fig. 14(h). Comparison of Computed H_2O Transmittance with High Resolution Laboratory Experimental Observations Characteristic of Atmospheric Paths (The conditions are listed in Table 8. The solid curve was obtained from the tabulation of experimental data in Ref. 9, and the dashed curve was calculated from the AFCRL atlas of spectroscopic parameters with the use of computer programs discussed in this report.)

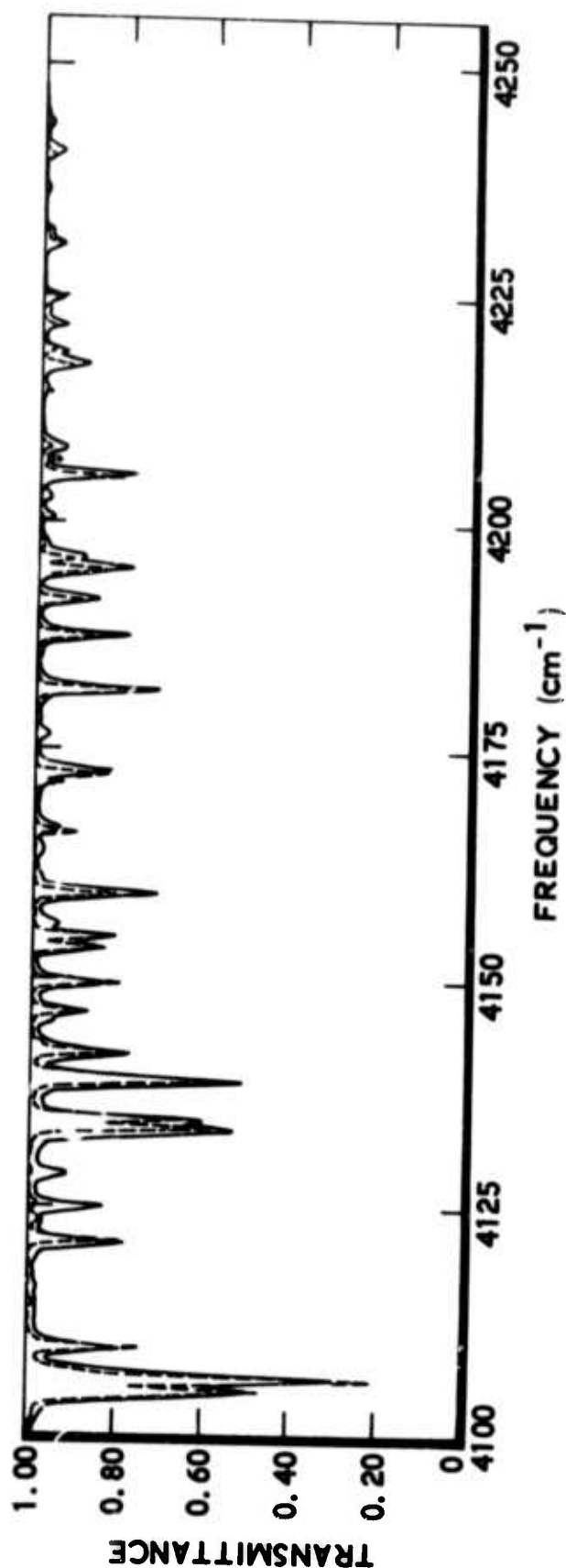


Fig. 14(i). Comparison of Computed H_2O Transmittance with High Resolution Laboratory Experimental Observations Characteristic of Atmospheric Paths (The conditions are listed in Table 8. The solid curve was obtained from the tabulation of experimental data in Ref. 9, and the dashed curve was calculated from the AFCRL atlas of spectroscopic parameters with the use of computer programs discussed in this report.)

in the atlas for this band. This sum has the value $1.46 \times 10^{-20} \text{ cm}^2 \text{ mole}^{-1} \text{ cm}^{-1}$. The listed strength for this band (Table 8, Ref. 2) is $7.99 \times 10^{-23} \text{ cm}^2 \text{ cm}^{-1} \text{ mole}^{-1}$, but J. E. A. Selby of AFCRL indicates the correct strength is $1.536 \times 10^{-23} \text{ cm}^2 \text{ mole}^{-1} \text{ cm}^{-1}$. In either case, the lines in our copy of the atlas appear to be too strong by about 3 orders of magnitude; this is confirmed by comparison with experimental data as indicated in Fig. 14(a). Recent recomputation of the spectrum with a revised atlas, in which the intensity of this band was corrected, has resulted in a spectrum that agrees much better with the experimental data.

The band strength discrepancy discussed above for the 010 to 030 band is by far the largest discrepancy found in comparing the band sums from the line atlas with the published band strengths. In view of the vast amount of data in this atlas, it is understandable how such an error could occur. Present experience indicates, however, the importance of comparing computed spectra with experimental spectra at sufficient resolution to identify individual spectral features.

D. HOT CO₂ PATH

The hot CO₂ experimental spectrum indicated by the solid line in Fig. 15 is taken from the work of F. S. Simmons.¹⁰ This spectrum has been replotted by hand from Fig. 6 of Ref. 10. The calculated spectrum indicated by the dashed line was obtained by convolving a triangular instrument function 5 cm^{-1} wide (FWHM) with the high resolution spectrum obtained from the AFCRL line atlas with the use of the INHOM computer program for the experimental conditions listed in Table 8. Note that this is a radiance spectrum rather than a transmittance spectrum such as those presented elsewhere in this section.

The excess radiance of the experimental spectrum compared to the calculated curve at low wave numbers is due to transitions not included in the line atlas because their lower levels are not significantly populated under atmospheric conditions. This defect is due to the application of the AFCRL

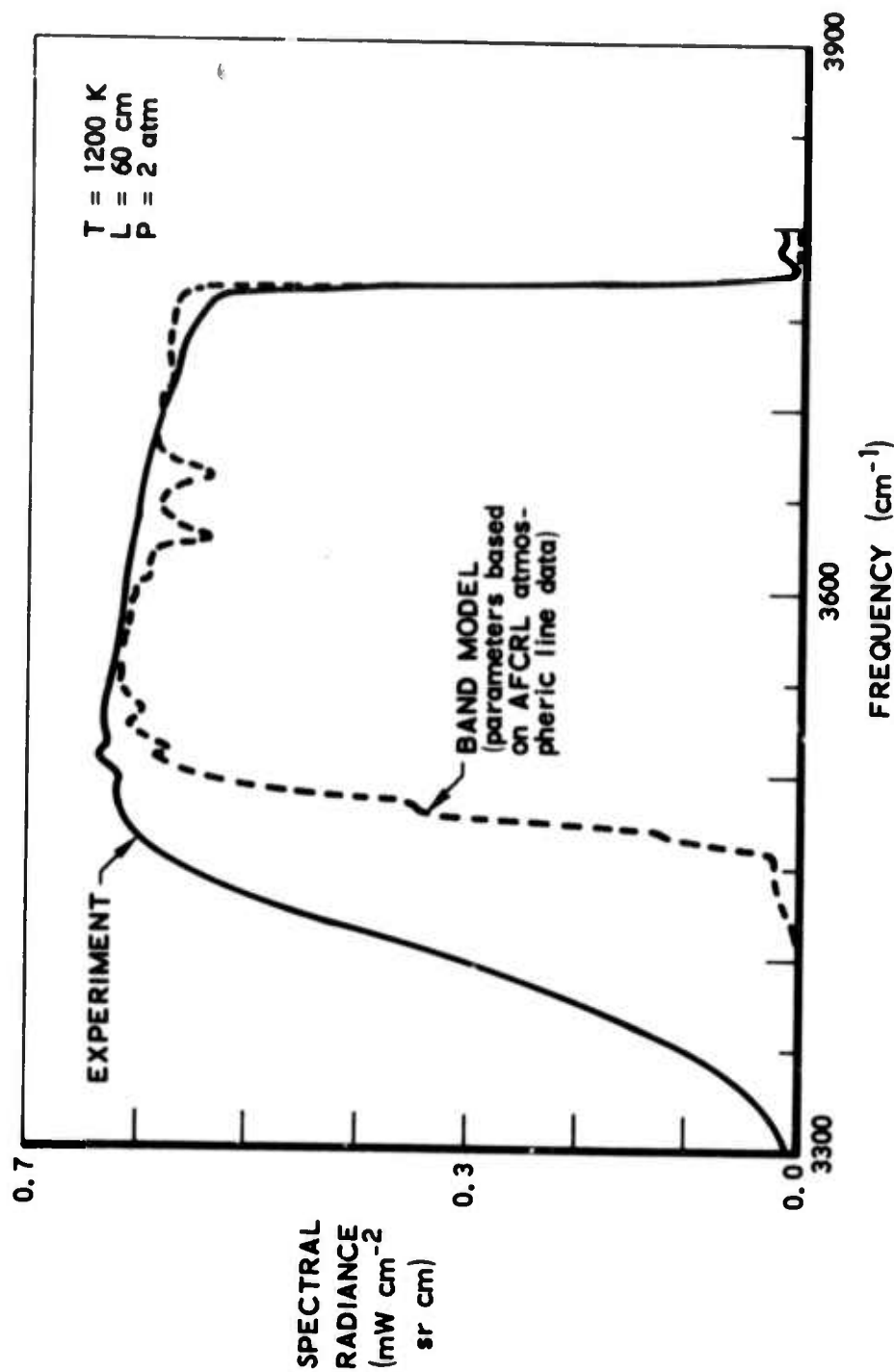


Fig. 15. Comparison of Computed CO_2 Radiance with Laboratory Observations at High Temperature (The dashed curve was calculated from the AFCRL atlas of spectroscopic parameters with the use of the computer programs discussed in this report. The solid curve was replotted from Ref. 10.)

atlas to conditions for which it was not constructed. The excess of the calculated radiance over the experimental at high wave numbers, on the other hand, is not understood, but perhaps represents a problem in the calibration of the experimental setup. Dips in the radiance in the calculated spectrum, which are not reproduced in the experimental spectrum, may be due to the use of a spectral slit width greater than 5 cm^{-1} in the determination of the experimental spectrum, or to transitions omitted from the line atlas.

In general, in this spectral region, the AFCRL atlas again appears correct for CO_2 except for the intentional omission of transitions arising from highly excited lower levels. These omissions can, of course, lead to serious problems in the wings of bands, as indicated in Fig. 15.

E. HOT H_2O PATH

The experimental spectrum represented by the solid line in Fig. 16 was obtained from the work of F. S. Simmons.¹¹ The curve illustrated was obtained from a photograph of Fig. 47 in Ref. 11 that was then transformed into a computer-compatible format by the method described in connection with the high resolution atmospheric CO_2 path. Here, in addition to a shift in the frequency scale, a 3-percent compression of the original wavelength scale was required to allow the position of the major features of the experimental spectrum to agree with the computed spectrum. The computed spectrum, indicated by the dashed line, was calculated by convolving a 7.5 cm^{-1} wide (FWHM) triangular instrumental function with the high resolution spectrum obtained with the INHOM Program from the AFCRL atlas for the experimental conditions listed in Table 8.

Agreement of the experimental and computed spectra is good for frequencies greater than about 3450 cm^{-1} . Around 4100 cm^{-1} there is an indication of the effect of omitted lines from highly excited states, but the difference is not large. Below 3450 cm^{-1} , the comparison is very poor. This is the result in large part of the erroneous line strengths assigned to the lines of the 010 to 130 band that lies in this spectral region, which was

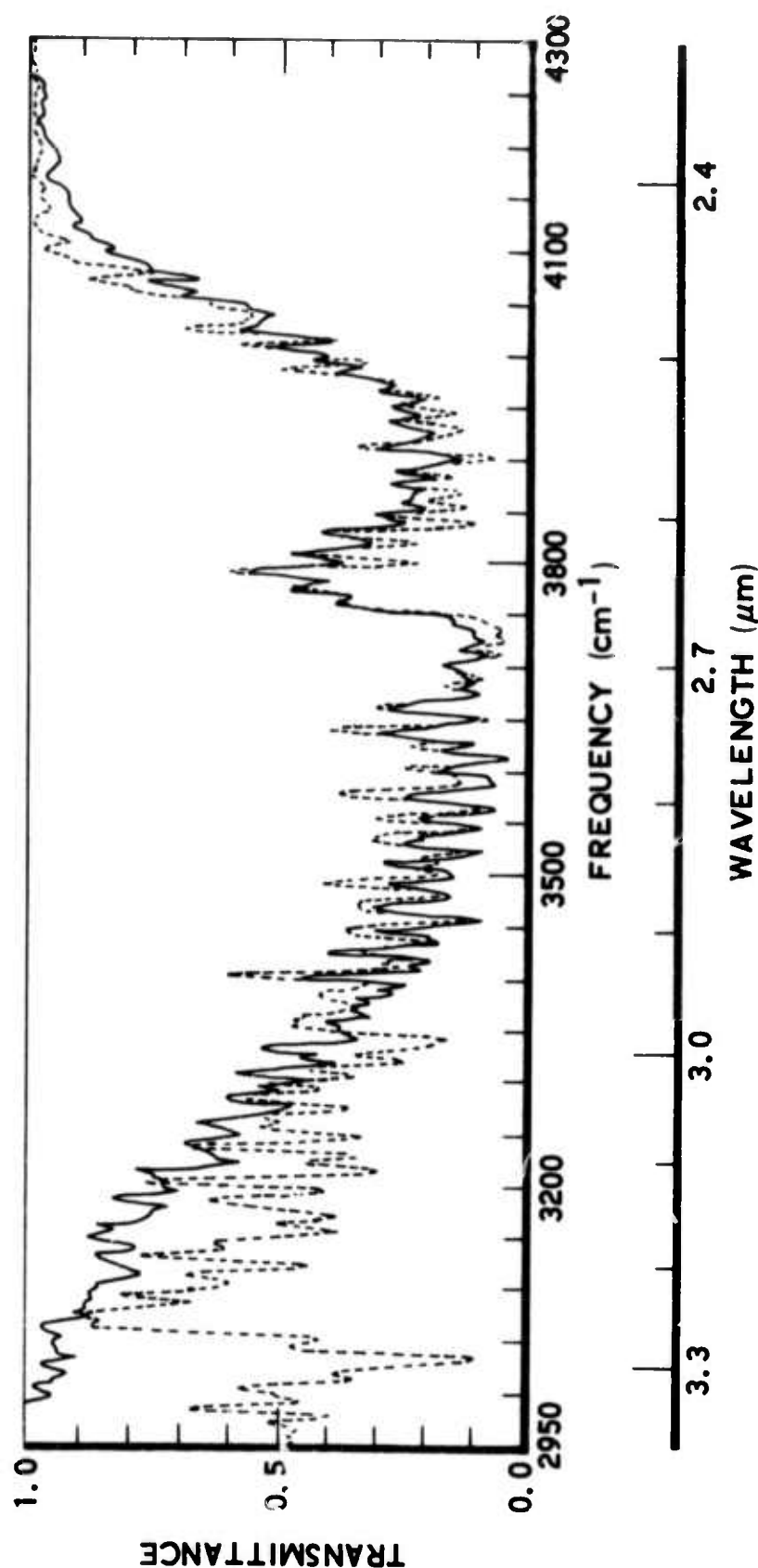


Fig. 16. Comparison of Computed H_2O Transmittance with Laboratory Experimental Observations at High Temperature (The conditions are listed in Table 8. The solid curve was obtained from a spectrum published in Ref. 11 by means discussed in the text. The dashed curve was calculated from the AFCRL atlas of spectroscopic parameters with the use of the computer programs discussed in this report.)

discussed previously. Several of these lines have lower energy levels of about 2000 cm^{-1} , so that increasing the temperature from 300 K to 1000 K results in an increase of about 3 orders of magnitude in the Boltzmann factor in the line strength. As a result, these lines are strong absorbers in this region. Because of the presence of these incorrect strong lines, no conclusions can be drawn about the applicability of our version of the AFCRL line atlas to calculation of the radiation from hot H_2O .

V. SUMMARY

- A program and associated procedures have been developed to compute high resolution spectra for inhomogeneous optical paths, including the conditions present in a missile plume. These programs and procedures are outlined in this report.
- These programs and procedures have been used with the AFCRL line atlas to demonstrate that ignoring the correlation of atmospheric absorption lines with source emission lines can lead to errors as large as 79 percent in the computed transmittance under some conditions.
- The AFCRL line atlas needs to have lines added to it from highly excited states to provide an adequate data base for the calculation of high temperature optical properties of gases.

APPENDIX

USER'S GUIDE TO INHOM

1. INTRODUCTION

The understanding of many atmospheric optical phenomena can be studied by modeling these optical effects with computer calculations. The INHOM Program, which is described here, may be used to calculate the transmittance and radiance of an optical path through an atmosphere which may or may not be homogeneous. This program is structured modularly so that, by replacing various modules in the program, almost any physical process that can be incorporated into a radiative transfer problem can be accommodated.

The programs have been written principally in FORTRAN-IV compatible with the Control Data Corporation (CDC) FTN compiler in use on the CDC 7600 computer at The Aerospace Corporation. A few routines, which must be very efficient or must perform functions not readily programmable in FORTRAN, have been written in the CDC assembly language COMPASS.

The first application of this program has been to compute infrared atmospheric transmittance and radiance under conditions typical of the lower atmosphere where the assumption of local thermodynamic equilibrium is valid and the individual spectral lines are pressure broadened. The basic spectroscopic input to these calculations is the atlas of line parameters prepared under the coordination of R. A. McClatchey at the Air Force Cambridge Research Laboratories.² The format of this input data is described in paragraph 3. The output of the program is a printed listing of computed transmittance and radiance together with a listing of various intermediate results. Transmittance/radiance results are also available in computer compatible format and may be saved on magnetic tape. The format of this output, described in paragraph 4, is compatible with the input requirements for the spectral analysis program SPECST already available (see Ref. 3, Section V).

Details of the specific calculation to be performed are controlled by computation step cards described in paragraph 2. A sample run is described in paragraph 5.

2. INHOM PROGRAM CONTROL

a. INTRODUCTION

The computations performed by the INHOM Program are controlled by a series of computation step cards. These cards are read as input data by the computer program after it has been called into execution.

Each computation of a spectrum is initiated by a SPECTRUM step card and results in the computation of a single spectrum. The physical parameters for which the spectrum is computed are specified by parameters on the SPECTRUM step card and the information available from other preceding step definition cards. All information input by step cards other than a SPECTRUM step card is retained unchanged by the program until it is superseded by the occurrence in the input stream of the same step definition with different parameters. In this way, it is possible to calculate spectra under varying physical conditions by respecifying only those variables that change rather than all the variables influencing the calculation.

b. STEP DEFINITION FORMAT

All computation step cards, except as explicitly noted in the detailed step descriptions, have the following properties in common.

- (1) The cards are free form in the sense that there is no rigid requirement that specifications begin in a particular card column or that they have a specific fixed field length. The beginning and length of fields are specified explicitly on the input cards by certain symbols and conventions.
- (2) The specification of each step must begin on a new card. In some cases, this may extend for more than one card.
- (3) Spelling is important. Only the combinations of letters and numbers listed in the detailed step descriptions are recognized. All other combinations will result in error messages to the user from the program. No blanks may be embedded within names and numerical values since a blank is used as a field delimiter.

- (4) The first word on the card, called a step definition word, indicates to the program what is to be done.
- (5) The order in which steps are specified preceding a SPECTRUM step is usually not important. When a SPECTRUM step is encountered, it computes a spectrum based on all the information specified to that point in the input stream.
- (6) For some steps, numerical parameters are required. These are input by a routine similar to an internal FORTRAN NAMELIST routine.
 - (a) The beginning of the parameter list is indicated by a left parenthesis.
 - (b) The parameters are specified in the format name = value. In the step descriptions when the value is indicated by nnn, a fixed point number is required. When the value is indicated by fff, a floating point number is required. If the decimal point is omitted from a floating point number, it will be assumed immediately to the right of the last digit.
 - (c) Specifications are separated by commas and terminated with a slash, /, or right parenthesis,).
 - (d) No blanks may be embedded in names or values, but they are permitted elsewhere.
 - (e) Parameter definition must begin on the first card of the step or definition and, unless stated otherwise, must be completed on that card.
 - (f) The parameters may be specified in any order.

c. DETAILED COMPUTATION STEP DEFINITION

TITLE

The contents of Columns 11 through 80 of this card are concatenated with the date on which the run was made. The resulting 80-character-long string is used whenever a title is needed in the printed listing. This string is also used to label the output spectrum put onto magnetic tape. A title remains unchanged until another TITLE step is encountered.

STOP

This step ends the run. Any step control cards remaining in that section of the input file are ignored.

ATMOSPHERE

This step specifies the input atmosphere through which the optical path will go. Two options are available: (1) The atmosphere may be specified in terms of altitude profiles of temperature, pressure, humidity, ozone concentration, and aerosol concentration. The GEOMETRY step is then required to convert this information into the physical parameters characterizing the optical path. (2) The physical parameters of the optical path may be defined directly. The atmosphere specified by this step remains in force until the next ATMOSPHERE step is encountered.

Step Card Format:

ATMOSPHERE	$\left\{ \begin{array}{c} \text{none} \\ \text{DIRECT} \\ \text{PRINT} \end{array} \right\}$	$\left\{ \begin{array}{c} \text{none} \\ \text{DIRECT} \\ \text{PRINT} \end{array} \right\}$
------------	--	--

The atmosphere is specified on the cards following the ATMOSPHERE card in a format depending on the option selected on the ATMOSPHERE card. If the word DIRECT appears on the card, the direct option will be used; otherwise, the altitude profile option will be assumed. If the word PRINT appears, the input atmosphere will be printed in the output listing; otherwise, it will not be printed.

(1) Altitude Profile Option

The first card following the ATMOSPHERE card contains in Columns 5 and 6 the number of layers in the atmosphere. This is also the number of cards to follow. A maximum of 81 layers may be specified. The atmospheric levels are assumed to be in ascending order of altitude. The format of each card specifying an individual atmospheric level is indicated in the following listing. All variables are floating-point real numbers.

Altitude Profile Atmosphere Input Level Specification Format

<u>Card Columns</u>	<u>Physical Quantity</u>	<u>Units</u>
1 - 6	Altitude	kilometers
7 - 16	Pressure	millibars
17 - 22	Temperature	Kelvin
23 - 32	Water Vapor Density	gm/m ³
33 - 42	Ozone Density	gm/m ³
43 - 56	Aerosol Number Density	particles/cm ³

(2) Direct Input Option

The cards following the ATMOSPHERE card contain the path length, molecular concentration, temperature, and pressure in each segment of the atmosphere through which the optical path passes. The input for each segment is a free form parameter list. Each segment specification begins on a new card and is indicated by a left parenthesis, (. Specification of that level continues until a right parenthesis,), is encountered. Specification of a single segment may be continued over several cards by starting a new card anywhere a comma is allowed in the free form parameter list. Segments are assumed to be specified in the order in which they will occur along the optical path. The first left parenthesis introduces the first segment of the optical path. This segment specification is terminated by the first right parenthesis. The next segment begins on the next card with a left parenthesis, and so on. The direct input option is terminated by: (a) completing a segment specification with a right parenthesis; and then (b) following this with one card, which may have any characters on it except a left parenthesis. The variable names recognized and the units associated with them are as follows:

<u>Variable Name</u>	<u>Physical Quantity</u>	<u>Units</u>
P = fff	Pressure	Millibars
T = fff	Temperature	Kelvin
WH2O = fff	Water Concentration	molecules/cm ²
WCO2 = fff	CO ₂ Concentration	molecules/cm ²
WO3 = fff	O ₃ Concentration	molecules/cm ²
WN2O = fff	N ₂ O Concentration	molecules/cm ²
WCH4 = fff	CH ₄ Concentration	molecules/cm ²
WCO = fff	CO Concentration	molecules/cm ²
WO2 = fff	O ₂ Concentration	molecules/cm ²
WHAZE = fff	Aerosol Concentration	particles/cm ²
DX = fff	Path Length in Segment	kilometers

COMPONENTS

This controls which gases are assumed to exist in the atmosphere. If gases are turned off here, the lines are never removed from the atlas and less computing time is required than if the concentration is set to zero.

Format:

COMPONENTS name $\begin{Bmatrix} \text{OFF} \\ \text{ON} \end{Bmatrix}$ name $\begin{Bmatrix} \text{OFF} \\ \text{ON} \end{Bmatrix}$

where name is one of the following words:

H2O
CO2
O3
N2O
CO
CH4
O2
HAZE
ALL

The OFF following one of these words tells the program to omit that component from the computation.

ON following one of these words includes that component in the computation.

ALL turns all of the components off or on depending on the word following.

Words must be separated by spaces, commas, or left parentheses, (. Initially all components are on.

GEOMETRY

This specifies the optical path followed by the radiation through the atmosphere. This step will convert an atmosphere, specified by the altitude profile option, into the parameters required for calculations along the optical path. If the ATMOSPHERE DIRECT option is used, there is no conversion to be performed and, therefore, data input with a GEOMETRY step are ignored. The actual conversion takes place when the computation is initiated by the SPECTRUM step, so the order of ATMOSPHERE and GEOMETRY steps in the input stream is unimportant. The GEOMETRY specified will continue to be used until another GEOMETRY card is encountered. Unless the ATMOSPHERE DIRECT step is specified, at least one GEOMETRY step must precede the first SPECTRUM step.

Refraction is ignored. The earth is assumed to be spherical with a radius of 6378.16 km. Impossible geometric paths are flagged. All possible geometric paths, including zenith angles greater than 90 deg, are believed to be handled correctly.

Format:

GEOMETRY (Parameters)

Parameters:

- BEGALT = fff is the beginning altitude in km for the path.
FINALT = fff is the final altitude in km for the path.
ZA = fff is the zenith angle of the optical path at the beginning point in degrees.
NLEVEL = nnn is the number of segments into which the path is broken. A maximum of 81 is allowed.
LNGPTH = 1 indicates for $ZA > 90$ deg that the longer of the two possible paths is to be considered. Any other value results in considering the shorter path. For $ZA \leq 90$ deg, this variable is ignored. The default value is zero.

PRINT

This controls the printing of auxiliary information. The print options remain in force until overridden by another PRINT step.

Format:

PRINT type $\left\{ \begin{array}{l} \text{ON} \\ \text{anything else} \end{array} \right\}$ type $\left\{ \begin{array}{l} \text{ON} \\ \text{anything else} \end{array} \right\}$

Type indicates the information desired for auxiliary output and ON enables that particular printing option. Any other word will turn that option off.

The types recognized are:

- ADDLINES Every time additional lines are extracted from the line atlas, they are listed.
WMATRIX Before the spectrum computation is initiated, the matrix of environmental parameters specifying the segments along the optical path will be printed.
SHAPE The line strength and line-broadening parameters to be used for each segment are printed.
DIVY The altitudes of the ends of the segments used for converting an atmosphere to a segmented path are printed.

These print options are initially set to OFF (no printing).

It should be noted that some other auxiliary printing options are controlled by parameters in certain step definitions.

SPECTRUM

This step initiates the computation of a spectrum. It is the one step that is required for every spectrum.

Format:

SPECTRUM (Parameters)

Parameters:

The first four parameters must be specified on every SPECTRUM step card. The other parameters are optional and will be reset to their default values for every computation unless otherwise specified.

- | | | | |
|-------|---|-----|---|
| BEG | = | fff | is the beginning frequency for which the spectrum is desired (cm^{-1}). |
| END | = | fff | is the ending frequency for which the spectrum is desired (cm^{-1}). |
| DNU | = | fff | is the step size by which frequency is stepped from BEG to END (cm^{-1}). |
| BOUND | = | fff | is the maximum distance away from a frequency for which lines are considered to contribute (cm^{-1}). |
| IPNT | = | 1 | causes the radiance and transmittance to be printed out. Other values cause no listing. The default is no listing. |
| ITRN | = | 0 | causes only the transmittance spectrum to be computed. This saves time and makes each output spectrum record contain twice the frequency interval. The default is zero and so both the radiance and transmittance are computed. |

If both radiance and transmittance are computed, the spectrum type (Table A-3, word 9) is LINE SPECT. If only transmittances are computed, the spectrum type is SPECTRUM.

3. LINE ATLAS FORMAT

The spectroscopic data required for the calculation of transmittance is stored on magnetic tape in the form of 80-character punched-card images. Each card image corresponds to one line, and up to 40 lines (card images) are stored in each block on the tape. The first word of each block contains an integer indicating the number of lines stored in that block. The lines are organized in an ascending order of frequency. For convenience in gaining access to the data, different spectral regions are separated into different files. These spectral regions and their associated file numbers are shown in Table A-1.

Table A-1. Frequency Range Covered by Each File on the Line Atlas Tape

File	Frequency Interval (cm^{-1})
1	0 - 500
2	500 - 1000
3	1000 - 2000
4	2000 - 5000
5	5000 - 10,000

Spectroscopic parameters needed for the calculation are listed in Table A-2 along with the fields on the card employed and the FORTRAN format associated with the field. For further details, consult Ref. 2.

At present, about 110,000 lines are available in the atlas. These include seven gases listed in Table A-2.

Table A-2. Parameters in Spectroscopic Line Atlas

Characters	FORTTRAN Format	Parameter	Units																
1 - 10	F10.3	Line center frequency	cm ⁻¹																
11 - 20	E10.3	Line strength at 296 K	cm ⁻¹ /(molecules cm ⁻²)																
21 - 25	F5.3	Line width parameter at 296 K	cm ⁻¹ /atmosphere																
26 - 35	F10.3	Energy level of lower state in transition	cm ⁻¹																
36 - 70	5A6, A5	Quantum numbers ^a	none																
71 - 73	I3	Date	none																
74 - 77	I4	Isotope ^a	none																
78 - 80	I3	Molecule indicated as follows:	none																
		<table><tr><th>Molecule</th><th>Code</th></tr><tr><td>H₂O</td><td>1</td></tr><tr><td>CO₂</td><td>2</td></tr><tr><td>O₃</td><td>3</td></tr><tr><td>N₂O</td><td>4</td></tr><tr><td>CO</td><td>5</td></tr><tr><td>CH₄</td><td>6</td></tr><tr><td>O₂</td><td>7</td></tr></table>	Molecule	Code	H ₂ O	1	CO ₂	2	O ₃	3	N ₂ O	4	CO	5	CH ₄	6	O ₂	7	
Molecule	Code																		
H ₂ O	1																		
CO ₂	2																		
O ₃	3																		
N ₂ O	4																		
CO	5																		
CH ₄	6																		
O ₂	7																		

^aThe detailed code depends on which molecule is involved (see Ref. 2).

4. COMPUTER COMPATIBLE OUTPUT FORMAT

The computed spectra are available in computer compatible format on file TAPE30. The format of this file is compatible with the input to SPECST, which is the spectral analysis program that is part of the Fourier spectroscopy computer package available at Aerospace.³

When the file is put on tape, it is 7-track 800-bpi odd parity. A spectrum may contain one or more logical records. The format of each logical record is shown in Table A-3. The length of every logical record in a single spectrum is the same, but the logical records in different files on the same tape may be of different lengths.

5. SAMPLE PROBLEM

A sample computer run is shown in Figs. A-1 and A-2. In Fig. A-1, a sample input deck is illustrated that uses the altitude profile method of specifying the atmosphere through which the radiation passes. Figure A-2 shows the computed results produced by INHOM on the basis of the input deck illustrated in Fig. A-1.

Table A-3. Logical Record Format for Spectrum Output Tapes

Word No.	Type	Description
1	Integer	File number. This begins with 1 for the first file on the tape.
2	Integer	The number of logical records in this file.
3	Integer	The logical record number, K, of this record. The first logical record is No. 1.
4	Floating	The frequency increment between data values in this file.
5	Floating	The frequency corresponding to the first value in the spectrum.
6	Floating	The maximum frequency for which a value is specified in the spectrum.
7	Floating	The minimum value in the spectrum. (For LINE SPECT spectra, this is zero.)
8	Floating	The maximum value in the spectrum. For LINE SPECT spectrum, it is the maximum value in the radiance spectrum.
9	Display	Spectrum type. SPECTRUM indicates a transmittance-only spectrum obtained by setting ITRN \neq 0 in the SPECTRUM step. LINE SPECT indicates the output consists of a transmittance and radiance spectrum.
10-17	Display	The title used to label the printout when the tape was originally generated.
18	Integer	NWRDS, the number of remaining words in this logical record, all of which are data words.
19 to NWRDS+18	Floating	The values of the spectrum. Details depend on the spectrum type. On multirecord files, it is the values $(K-1)*N + 1$ to $K*N$ where N depends on the spectrum type (defined below) and K comes from Word 3. For SPECTRUM type spectra, $N = \text{NWRDS}$. All of the values are spectral values in ascending order of frequency. For LINE SPECT type spectra, $N = \text{NWRDS}/2$. Words 1 to N of the values section are the transmittance values in ascending order of frequency. Words N+1 to NWRDS are the radiance values in ascending order of frequency.

```

FINISHED LINE SPECTRUM CALCULATION RUN
TITLE TROPICAL MODEL ATMOSPHERE
ATMOSPHERE PRINT
33
0.0 1.0 1.3E+03 300.0 1.9E+01 5.0 2.8300E+03
1.0 9.040E+02 294.0 1.3E+01 5.0 1.2451E+03
2.0 8.050E+02 288.0 9.3E+00 5.0 5.3740E+02
3.0 7.150E+02 284.0 4.7E+00 5.0 5.2570E+02
4.0 6.430E+02 277.0 2.2E+00 4.0 1.1930E+02
5.0 5.590E+02 270.0 1.0E+00 4.0 8.9920E+01
6.0 4.430E+02 254.0 0.3E+00 4.0 6.3410E+01
7.0 3.320E+02 257.0 0.1E+00 4.0 5.8930E+01
8.0 3.370E+02 250.0 0.1E+00 3.0 6.0730E+01
9.0 3.230E+02 244.0 0.1E+00 3.0 5.8220E+01
10.0 2.860E+02 237.0 0.1E+00 3.0 5.6790E+01
11.0 2.470E+02 230.0 0.1E+00 4.0 5.3200E+01
12.0 2.130E+02 224.0 0.1E+00 4.0 5.5890E+01
13.0 1.820E+02 217.0 0.1E+00 4.0 5.1590E+01
14.0 1.560E+02 210.0 0.1E+00 4.0 5.0520E+01
15.0 1.320E+02 204.0 0.1E+00 4.0 4.7470E+01
16.0 1.110E+02 197.0 0.1E+00 4.0 4.5140E+01
17.0 9.370E+01 195.0 0.1E+00 6.0 4.4600E+01
18.0 7.390E+01 199.0 0.1E+00 9.0 4.3170E+01
19.0 6.560E+01 203.0 0.1E+00 1.0 3.6360E+01
20.0 5.650E+01 207.0 0.1E+00 1.0 2.6890E+01
21.0 4.830E+01 211.0 0.1E+00 2.0 1.9350E+01
22.0 4.090E+01 215.0 0.1E+00 2.0 1.4560E+01
23.0 3.500E+01 217.0 0.1E+00 3.0 1.1140E+01
24.0 3.000E+01 219.0 0.1E+00 3.0 8.8310E+00
25.0 2.570E+01 221.0 0.1E+00 3.0 7.4340E+00
30.0 1.220E+01 232.0 0.1E+00 2.0 2.2390E+00
35.0 6.000E+00 253.0 0.1E+00 1.0 5.8930E-01
40.0 3.000E+00 254.0 0.1E+00 1.0 1.5510E-01
45.0 1.000E+00 255.0 0.1E+00 1.0 4.0840E-02
50.0 0.500E+00 270.0 0.1E+00 6.0 1.0780E-02
55.0 0.250E+00 219.0 0.1E+00 1.0 5.5530E-03
60.0 0.125E+00 210.0 0.1E+00 1.0 1.9700E-03
TITLE 20 KM TO SPACE TRANSMITTANCE
PRINT MATRIX ON
COMPONENTS ALL ON
GEOMETRY (REGALT=20.0, FINALT=100.0, NLEVEL=5, ZA = 75.0)
SPECTRUM (BEG=3560.0, END=3562.0, DNU=0.01, BOUND = 10.0, IPNT=1)
STOP

```

Fig. A-1. Sample Input Deck for INHOM Program Employing the Altitude Profile Method of Specifying the Atmosphere Through Which the Optical Path Goes

G9/23/74 NUMBER	TROPICAL ALTITUDE (KM)	MODEL ATMOSPHERE PRESSURE (MB)	TEMP. (K)	WATER (GM/H ²)	OZONE (GM/H ²)	AEROSOL (PARTS/CM ³)
1	0.00	1013.00	300.00	190000E+02	560000E-04	283000E+04
2	1.00	904.00	294.00	130000E+01	560000E-04	124500E+04
3	2.00	805.00	288.00	930000E+01	540000E-04	537400E+03
4	3.00	715.00	284.00	570000E+01	510000E-04	225700E+03
5	4.00	633.00	277.00	220000E+01	450000E-04	119200E+02
6	5.00	559.00	264.00	150000E+00	430000E-04	834000E+02
7	6.00	492.00	257.00	870000E+00	390000E-04	589300E+02
8	7.00	432.00	247.00	450000E+00	390000E-04	507300E+02
9	8.00	373.00	237.00	220000E+01	390000E-04	562200E+02
10	9.00	329.00	230.00	120000E+00	430000E-04	553200E+02
11	10.00	286.00	217.00	700000E+00	450000E-04	515900E+02
12	11.00	247.00	210.00	300000E+00	470000E-04	505200E+02
13	12.00	213.00	204.00	160000E+00	470000E-04	474700E+02
14	13.00	182.00	197.00	800000E+00	490000E-04	451400E+02
15	14.00	156.00	194.00	400000E+00	490000E-04	436000E+02
16	15.00	132.00	195.00	200000E+00	490000E-04	431600E+02
17	16.00	111.70	199.00	100000E+00	490000E-04	436900E+02
18	17.00	93.90	203.00	500000E+00	490000E-04	435500E+02
19	18.00	86.50	207.00	250000E+00	490000E-04	435500E+02
20	19.00	80.90	211.00	120000E+00	490000E-04	435500E+02
21	20.00	76.00	215.00	600000E+00	490000E-04	435500E+02
22	21.00	71.00	217.00	300000E+00	490000E-04	435500E+02
23	22.00	66.00	219.00	150000E+00	490000E-04	435500E+02
24	23.00	61.00	221.00	700000E+00	490000E-04	435500E+02
25	24.00	56.00	223.00	360000E+00	490000E-04	435500E+02
26	25.00	51.00	225.00	190000E+00	490000E-04	435500E+02
27	26.00	46.00	227.00	100000E+00	490000E-04	435500E+02
28	27.00	41.00	229.00	500000E+00	490000E-04	435500E+02
29	28.00	36.00	231.00	250000E+00	490000E-04	435500E+02
30	29.00	31.00	233.00	120000E+00	490000E-04	435500E+02
31	30.00	26.00	235.00	600000E+00	490000E-04	435500E+02
32	31.00	21.00	237.00	300000E+00	490000E-04	435500E+02
33	32.00	16.00	239.00	150000E+00	490000E-04	435500E+02
34	33.00	11.00	241.00	700000E+00	490000E-04	435500E+02
35	34.00	6.00	243.00	360000E+00	490000E-04	435500E+02
36	35.00	1.00	245.00	190000E+00	490000E-04	435500E+02
37	36.00	0.00	247.00	100000E+00	490000E-04	435500E+02
38	37.00	0.00	249.00	500000E+00	490000E-04	435500E+02
39	38.00	0.00	251.00	250000E+00	490000E-04	435500E+02
40	39.00	0.00	253.00	120000E+00	490000E-04	435500E+02
41	40.00	0.00	255.00	600000E+00	490000E-04	435500E+02
42	41.00	0.00	257.00	300000E+00	490000E-04	435500E+02
43	42.00	0.00	259.00	150000E+00	490000E-04	435500E+02
44	43.00	0.00	261.00	700000E+00	490000E-04	435500E+02
45	44.00	0.00	263.00	360000E+00	490000E-04	435500E+02
46	45.00	0.00	265.00	190000E+00	490000E-04	435500E+02
47	46.00	0.00	267.00	100000E+00	490000E-04	435500E+02
48	47.00	0.00	269.00	500000E+00	490000E-04	435500E+02
49	48.00	0.00	271.00	250000E+00	490000E-04	435500E+02
50	49.00	0.00	273.00	120000E+00	490000E-04	435500E+02
51	50.00	0.00	275.00	600000E+00	490000E-04	435500E+02
52	51.00	0.00	277.00	300000E+00	490000E-04	435500E+02
53	52.00	0.00	279.00	150000E+00	490000E-04	435500E+02
54	53.00	0.00	281.00	700000E+00	490000E-04	435500E+02
55	54.00	0.00	283.00	360000E+00	490000E-04	435500E+02
56	55.00	0.00	285.00	190000E+00	490000E-04	435500E+02
57	56.00	0.00	287.00	100000E+00	490000E-04	435500E+02
58	57.00	0.00	289.00	500000E+00	490000E-04	435500E+02
59	58.00	0.00	291.00	250000E+00	490000E-04	435500E+02
60	59.00	0.00	293.00	120000E+00	490000E-04	435500E+02
61	60.00	0.00	295.00	600000E+00	490000E-04	435500E+02
62	61.00	0.00	297.00	300000E+00	490000E-04	435500E+02
63	62.00	0.00	299.00	150000E+00	490000E-04	435500E+02
64	63.00	0.00	301.00	700000E+00	490000E-04	435500E+02
65	64.00	0.00	303.00	360000E+00	490000E-04	435500E+02
66	65.00	0.00	305.00	190000E+00	490000E-04	435500E+02
67	66.00	0.00	307.00	100000E+00	490000E-04	435500E+02
68	67.00	0.00	309.00	500000E+00	490000E-04	435500E+02
69	68.00	0.00	311.00	250000E+00	490000E-04	435500E+02
70	69.00	0.00	313.00	120000E+00	490000E-04	435500E+02
71	70.00	0.00	315.00	600000E+00	490000E-04	435500E+02
72	71.00	0.00	317.00	300000E+00	490000E-04	435500E+02
73	72.00	0.00	319.00	150000E+00	490000E-04	435500E+02
74	73.00	0.00	321.00	700000E+00	490000E-04	435500E+02
75	74.00	0.00	323.00	360000E+00	490000E-04	435500E+02
76	75.00	0.00	325.00	190000E+00	490000E-04	435500E+02
77	76.00	0.00	327.00	100000E+00	490000E-04	435500E+02
78	77.00	0.00	329.00	500000E+00	490000E-04	435500E+02
79	78.00	0.00	331.00	250000E+00	490000E-04	435500E+02
80	79.00	0.00	333.00	120000E+00	490000E-04	435500E+02
81	80.00	0.00	335.00	600000E+00	490000E-04	435500E+02
82	81.00	0.00	337.00	300000E+00	490000E-04	435500E+02
83	82.00	0.00	339.00	150000E+00	490000E-04	435500E+02
84	83.00	0.00	341.00	700000E+00	490000E-04	435500E+02
85	84.00	0.00	343.00	360000E+00	490000E-04	435500E+02
86	85.00	0.00	345.00	190000E+00	490000E-04	435500E+02
87	86.00	0.00	347.00	100000E+00	490000E-04	435500E+02
88	87.00	0.00	349.00	500000E+00	490000E-04	435500E+02
89	88.00	0.00	351.00	250000E+00	490000E-04	435500E+02
90	89.00	0.00	353.00	120000E+00	490000E-04	435500E+02
91	90.00	0.00	355.00	600000E+00	490000E-04	435500E+02
92	91.00	0.00	357.00	300000E+00	490000E-04	435500E+02
93	92.00	0.00	359.00	150000E+00	490000E-04	435500E+02
94	93.00	0.00	361.00	700000E+00	490000E-04	435500E+02
95	94.00	0.00	363.00	360000E+00	490000E-04	435500E+02
96	95.00	0.00	365.00	190000E+00	490000E-04	435500E+02
97	96.00	0.00	367.00	100000E+00	490000E-04	435500E+02
98	97.00	0.00	369.00	500000E+00	490000E-04	435500E+02
99	98.00	0.00	371.00	250000E+00	490000E-04	435500E+02
100	99.00	0.00	373.00	120000E+00	490000E-04	435500E+02
101	100.00	0.00	375.00	600000E+00	490000E-04	435500E+02
102	101.00	0.00	377.00	300000E+00	490000E-04	435500E+02
103	102.00	0.00	379.00	150000E+00	490000E-04	435500E+02
104	103.00	0.00	381.00	700000E+00	490000E-04	435500E+02
105	104.00	0.00	383.00	360000E+00	490000E-04	435500E+02
106	105.00	0.00	385.00	190000E+00	490000E-04	435500E+02
107	106.00	0.00	387.00	100000E+00	490000E-04	435500E+02
108	107.00	0.00	389.00	500000E+00	490000E-04	435500E+02
109	108.00	0.00	391.00	250000E+00	490000E-04	435500E+02
110	109.00	0.00	393.00	120000E+00	490000E-04	435500E+02
111	110.00	0.00	395.00	600000E+00	490000E-04	435500E+02
112	111.00	0.00	397.00	300000E+00	490000E-04	435500E+02
113	112.00	0.00	399.00	150000E+00	490000E-04	435500E+02
114	113.00	0.00	401.00	700000E+00	490000E-04	435500E+02
115	114.00	0.00	403.00	360000E+00	490000E-04	435500E+02
116	115.00	0.00	405.00	190000E+00	490000E-04	435500E+02
117	116.00	0.00	407.00	100000E+00	490000E-04	435500E+02
118	117.00	0.00	409.00	500000E+00	490000E-04	435500E+02
119	118.00	0.00	411.00	250000E+00	490000E-04	435500E+02
120	119.00	0.00	413.00	120000E+00	490000E-04	435500E+02
121	120.00	0.00	415.00	600000E+00	490000E-04	435500E+02
122	121.00	0.00	417.00	300000E+00	490000E-04	435500E+02
123	122.00	0.00	419.00	150000E+00	490000E-04	435500E+02
124	123.00	0.00	421.00	700000E+00	490000E-04	435500E+02
125	124.00	0.00	423.00	360000E+00	490000E-04	435500E+02
126	125.00	0.00	425.00	190000E+00	490000E-04	435500E+02
127	126.00	0.00	427.00	100000E+00	490000E-04	435500E+02
128	127.00	0.00	429.00	500000E+00	490000E-04	435500E+02
129	128.00	0.00	431.00	250000E+00	490000E-04	435500E+02
130	129.00	0.00	433.00	120000E+00	490000E-04	435500E+02
131	130.00	0.00	435.00	600000E+00	490000E-04	435500E+02
132	131.00	0.00	437.00	300000E+00	490000E-04	435500E+02
133	132.00	0.00	439.00	150000E+00	490000E-04	435500E+02
134	133.00	0.00	441.00	700000E+00	490000E-04	435500E+02
135	134.00	0.00	443.00	360000E+00	490000E-04	435500E+02
136	135.00	0.00	445.00	190000E+00	490000E-04	435500E+02
137	136.00	0.00	447.00	100000E+00	490000E-04	435500E+02
138	137.00	0.00	449.00	500000E+00	490000E-04	435500E+02
139	138.00	0.00	451.00	250000E+00	490000E-04	435500E+02
1						

Fig. A-2. Spectrum Computed and Listing Generated by the INHOM Program in Response to the Input Deck Shown in Fig. A-1 (Continued)

Fig. A-2. Spectrum Computed and Listing Generated by the INHOM Program in Response to the Input Deck Shown in Fig. A-1 (Continued)

Fig. A-2. Spectrum Computed and Listing Generated by the INHOM Program in Response to the Input Deck Shown in Fig. A-1 (Concluded)

REFERENCES

1. S. J. Young, Band Model Calculations of Atmospheric Transmittance for Hot Gas Line Emission Sources, TR-0075(5647)-1, The Aerospace Corporation, El Segundo, California (in preparation, June 1974).
2. R. A. McClatchey, W. S. Benedict, S. A. Clough, D. E. Burch, R. F. Calfee, K. Fox, L. S. Rothman, and J. S. Garing, AFCRL Atmospheric Absorption Line Parameters Compilation, Environmental Research Paper 434, AFCRL-TR-73-0096, Air Force Cambridge Research Laboratories, Mass. (26 January 1973).
3. C. M. Randall, User's Guide to Computer Programs for Fourier Spectroscopy, TR-0073(9260-01)-8, The Aerospace Corporation, El Segundo, California (30 November 1972).
4. G. Herzberg, Molecular Spectra and Molecular Structure, Van Nostrand Reinhold Company, New York, New York (1945), p. 501.
5. C. B. Ludwig, W. Malkmus, J. E. Reardon, and J. A. L. Thomson, Handbook of Infrared Radiation from Combustion Gases, NASA Special Publication NASA SP-3080 (1973).
6. R. A. McClatchey, R. W. Fenn, J. E. A. Selby, F. E. Volz, and J. S. Garing, Optical Properties of the Atmosphere (Third Ed.), Environmental Research Paper No. 411, AFCRL-72-0497, Air Force Cambridge Research Laboratories, Mass. (24 August 1972).
7. J. E. A. Selby and R. A. McClatchey, Atmospheric Transmittance from 0.25 to 28.5 μ m: Computer Code LOWTRAN2, Environmental Research Paper No. 427, AFCRL-72-0745, Air Force Cambridge Research Laboratories, Mass. (29 December 1972).
8. D. E. Burch, D. A. Gryvnak, and R. R. Patty, Absorption by CO₂ Between 3100 and 4100 cm^{-1} (2.44 - 3.22 Microns), U-4132, Aeronutronic Division of Philco-Ford, Newport Beach, California (30 April 1968).
9. D. E. Burch, D. A. Gryvnak, and R. R. Patty, Absorption by H₂O Between 2800 and 4500 cm^{-1} (2.7 Micron Region), U-3202, Aeronutronic Division of Philco-Ford, Newport Beach, California (30 September 1965).

10. F. S. Simmons, H. Y. Yamada, and C. B. Arnold, Measurements of Temperature Profiles in Hot Gases by Emission-Absorption Spectroscopy, University of Michigan Report WRL 8962-18-F, NASA CR-77491, Willow Run Laboratories (April 1969).
11. F. S. Simmons, C. B. Arnold, and D. H. Smith, Studies of Infrared Radiative Transfer in Hot Gases 1: Spectral Absorptance Measurements in the 2.7 μ H₂O Bands, University of Michigan Report 4613-91-T, Willow Run Laboratories (August 1965).

LABORATORY OPERATIONS

The Laboratory Operations of The Aerospace Corporation is conducting experimental and theoretical investigations necessary for the evaluation and application of scientific advances to new military concepts and systems. Versatility and flexibility have been developed to a high degree by the laboratory personnel in dealing with the many problems encountered in the nation's rapidly developing space and missile systems. Expertise in the latest scientific developments is vital to the accomplishment of tasks related to these problems. The laboratories that contribute to this research are:

Aerophysics Laboratory: Launch and reentry aerodynamics, heat transfer, reentry physics, chemical kinetics, structural mechanics, flight dynamics, atmospheric pollution, and high-power gas lasers.

Chemistry and Physics Laboratory: Atmospheric reactions and atmospheric optics, chemical reactions in polluted atmospheres, chemical reactions of excited species in rocket plumes, chemical thermodynamics, plasma and laser-induced reactions, laser chemistry, propulsion chemistry, space vacuum and radiation effects on materials, lubrication and surface phenomena, photo-sensitive materials and sensors, high precision laser ranging, and the application of physics and chemistry to problems of law enforcement and biomedicine.

Electronics Research Laboratory: Electromagnetic theory, devices, and propagation phenomena, including plasma electromagnetics; quantum electronics, lasers, and electro-optics; communication sciences, applied electronics, semiconducting, superconducting, and crystal device physics, optical and acoustical imaging; atmospheric pollution; millimeter wave and far-infrared technology.

Materials Sciences Laboratory: Development of new materials; metal matrix composites and new forms of carbon; test and evaluation of graphite and ceramics in reentry; spacecraft materials and electronic components in nuclear weapons environment; application of fracture mechanics to stress corrosion and fatigue-induced fractures in structural metals.

Space Physics Laboratory: Atmospheric and ionospheric physics, radiation from the atmosphere, density and composition of the atmosphere, aurorae and airglow; magnetospheric physics, cosmic rays, generation and propagation of plasma waves in the magnetosphere; solar physics, studies of solar magnetic fields; space astronomy, x-ray astronomy; the effects of nuclear explosions, magnetic storms, and solar activity on the earth's atmosphere, ionosphere, and magnetosphere; the effects of optical, electromagnetic, and particulate radiations in space on space systems.

THE AEROSPACE CORPORATION
El Segundo, California